LETTER

doi:10.1038/nature12979

IL-35-producing B cells are critical regulators of immunity during autoimmune and infectious diseases

Ping Shen[1]*, Toralf Roch[1]†*, Vicky Lampropoulou[1], Richard A. O'Connor[2], Ulrik Stervbo[1], Ellen Hilgenberg[1], Stefanie Ries[1], Van Duc Dang[1], Yarúa Jaimes[1], Capucine Daridon[1,3], Rui Li[4], Luc Jouneau[5], Pierre Boudinot[5], Siska Wilantri[1], Imme Sakwa[1], Yusei Miyazaki[4], Melanie D. Leech[2], Rhoanne C. McPherson[2], Stefan Wirtz[6], Markus Neurath[6], Kai Hoehlig[1], Edgar Meinl[7], Andreas Grützkau[1], Joachim R. Grün[1], Katharina Horn[1], Anja A. Kühl[8], Thomas Dörner[1,3], Amit Bar-Or[4], Stefan H. E. Kaufmann[9], Stephen M. Anderton[2] & Simon Fillatreau[1]

B lymphocytes have critical roles as positive and negative regulators of immunity. Their inhibitory function has been associated primarily with interleukin 10 (IL-10) because B-cell-derived IL-10 can protect against autoimmune disease and increase susceptibility to pathogens[1,2]. Here we identify IL-35-producing B cells as key players in the negative regulation of immunity. Mice in which only B cells did not express IL-35 lost their ability to recover from the T-cell-mediated demyelinating autoimmune disease experimental autoimmune encephalomyelitis (EAE). In contrast, these mice displayed a markedly improved resistance to infection with the intracellular bacterial pathogen *Salmonella enterica* serovar Typhimurium as shown by their superior containment of the bacterial growth and their prolonged survival after primary infection, and upon secondary challenge, compared to control mice. The increased immunity found in mice lacking IL-35 production by B cells was associated with a higher activation of macrophages and inflammatory T cells, as well as an increased function of B cells as antigen-presenting cells (APCs). During *Salmonella* infection, IL-35- and IL-10-producing B cells corresponded to two largely distinct sets of surface-IgM^{+} CD138^{hi}TACI^{+}CXCR4^{+}CD1d^{int}Tim1^{int} plasma cells expressing the transcription factor Blimp1 (also known as Prdm1). During EAE, CD138^{+} plasma cells were also the main source of B-cell-derived IL-35 and IL-10. Collectively, our data show the importance of IL-35-producing B cells in regulation of immunity and highlight IL-35 production by B cells as a potential therapeutic target for autoimmune and infectious diseases. This study reveals the central role of activated B cells, particularly plasma cells, and their production of cytokines in the regulation of immune responses in health and disease.

The inhibitory activities of B cells involve their production of IL-10, which in mice can protect from autoimmunity but impair resistance to infection[3–6]. Such suppressive function could be relevant to human diseases. A defect in IL-10 secretion by B cells was observed in patients with multiple sclerosis and type 1 diabetes[7,8]. Furthermore, B-cell depletion therapy had deleterious effects in some patients with multiple sclerosis or ulcerative colitis[9,10], and led to ulcerative colitis or psoriasis in patients with Graves' disease or rheumatoid arthritis, respectively[11,12]. These effects were probably not all owing to a loss of IL-10-producing B cells. Mouse B cells could inhibit immunity independently of IL-10 (refs 13, 14). However, no mediator to account for this has been characterized. There is an urgent need to identify additional factors mediating regulatory functions of B cells.

B cells require activation to exert suppressive activity and Toll-like receptors (TLR) are critical in this process. Mice with deficiencies in both TLR2 and TLR4 restricted to B cells developed an exacerbated EAE after immunization with the encephalitogenic peptide from myelin oligodendrocyte glycoprotein (MOG_{35-55})[15]. Using mice with single deficiencies in these TLR restricted to B cells ($B^{Tlr2^{-/-}}$ and $B^{Tlr4^{-/-}}$ mice, respectively), we found that TLR4 was the most critical for B-cell-mediated suppression in EAE (Fig. 1a and Extended Data Fig. 1a). With our previous studies[3], these results establish TLR4 and CD40 as receptors essential for the regulatory function of B cells in EAE. CD40 also contributes to the protective roles of B cells in ulcerative colitis and arthritis[4,5].

IL-10 production by B cells is required for recovery from EAE[3]. Naive B cells produced IL-10 after TLR4 engagement, but not upon co-stimulation by TLR4 plus CD40 (Fig. 1b and Extended Data Fig. 1b). To identify additional suppressive factor(s) produced upon TLR4 plus CD40 stimulation, we performed Affymetrix array analyses on (1) naive B cells, (2) B cells activated by TLR4 and (3) B cells activated by TLR4 plus CD40, and focused on genes coding for secreted molecules (Extended Data Fig. 1c). Among the genes differentially expressed, of interest was Epstein-Barr virus-induced gene 3 (*Ebi3*), a member of the IL-12 cytokine family that can dimerize with p28 or p35 to generate IL-27 or IL-35, respectively, which both have suppressive functions[16–19]. B cells did not express *p40* (also known as *Il12b*) messenger RNA, highlighting its cell-type specific expression pattern[20], but constitutively transcribed *p35* (also known as *Il12a*) (Extended Data Fig. 1d). In fact, B cells were the main source of *p35* mRNA in secondary lymphoid tissues (Fig. 1d). B cells upregulated expression of *p35* and *Ebi3* mRNA, as well as EBI3 protein upon activation by TLR4 plus CD40, which was further increased upon B-cell receptor for antigen (BCR) engagement, suggesting they could secrete IL-35 (Fig. 1e and Extended Data Fig. 1). This was confirmed by co-immunoprecipitation using supernatants from TLR4 plus CD40-activated B cells (Fig. 1f). We conclude that B cells can secrete IL-35 after activation by TLR4 plus CD40.

To evaluate the role of IL-35 expression by B cells during EAE, we used mice with a B-cell-restricted deficiency in p35 ($B^{p35^{-/-}}$), or EBI3 ($B^{Ebi3^{-/-}}$), or control mice with wild-type B cells (B^{WT}). We also used mice in which B cells could not express p40 ($B^{p40^{-/-}}$), or p28 ($B^{p28^{-/-}}$), because p35 can dimerize with p40 to form IL-12, and EBI3 can associate with p28 to form IL-27. B cells secreted p28 after activation (Extended Data Fig. 1j). $B^{p35^{-/-}}$ and $B^{Ebi3^{-/-}}$ mice developed exacerbated EAE, whereas $B^{p40^{-/-}}$ and $B^{p28^{-/-}}$ mice had disease courses similar

[1]Deutsches Rheuma-Forschungszentrum, a Leibniz Institute, Charitéplatz 1, 10117 Berlin, Germany. [2]University of Edinburgh, Centre for Inflammation Research and Centre for Multiple Sclerosis Research, Queen's Medical Research Institute, Edinburgh EH16 4TJ, UK. [3]Charité Universitätsmedizin Berlin, CC12, Department of Medicine/Rheumatology and Clinical Immunology, 10117 Berlin, Germany. [4]Neuroimmunology Unit, Montreal Neurological Institute and Hospital, McGill University, Montreal, Quebec H3A2B4, Canada. [5]Virologie et Immunologie Moléculaires, INRA, 78352 Jouy-en-Josas, France. [6]Medical Clinic 1, Kussmaul Campus for Medical Research, University of Erlangen-Nürnberg, 91054 Erlangen, Germany. [7]Institut für Klinische Neuroimmunologie Klinikum der Ludwig-Maximilians-Universität München, 81377 München, Germany. [8]Immunpathologie, Research Center ImmunoSciences, 12203 Berlin, Germany. [9]Max Planck Institute of Infection Biology, Department of Immunology, Charitéplatz 1, 10117 Berlin, Germany. †Present address: Institute of Biomaterial Science, Helmholtz-Zentrum Geesthacht, Centre for Materials and Coastal Research, Kantstraße 55, 14513 Teltow, Germany.
*These authors contributed equally to this work.

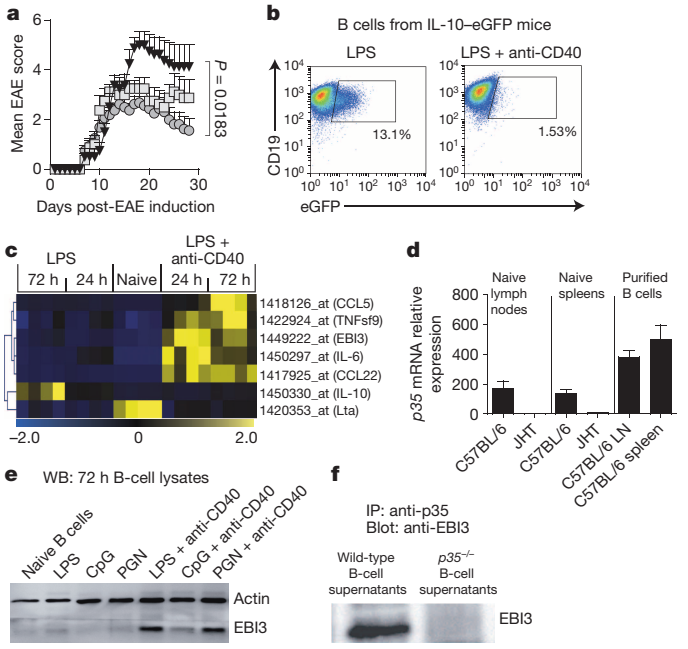

Figure 1 | B cells secrete IL-35 upon activation by TLR4 and CD40. **a**, EAE was induced in $B^{Tlr2^{-/-}}$ (grey squares, $n = 8$), $B^{Tlr4^{-/-}}$ (black triangles, $n = 8$) and B^{WT} mice (grey circles, $n = 16$). Data show clinical EAE scores from two independent experiments (mean ± s.e.m.). Cumulative disease scores were compared using two-tailed unpaired *t*-test. **b**, Splenic B cells from IL-10–eGFP (knock-in of eGFP at *Il10* locus) mice were stimulated for 72 h with LPS (1 μg ml^{-1}) or LPS (1 μg ml^{-1}) plus anti-CD40 (10 μg ml^{-1}), and eGFP expression was measured by flow cytometry. Plots show eGFP expression by live CD19$^+$ cells. Results are representative of three independent experiments. **c**, Hierarchical cluster analysis of secreted factors differentially expressed between B cells activated with LPS or LPS plus anti-CD40 (Pearson correlation with average linkage). Affymetrix microarrays were performed in quadruplicates. Gene expression levels are shown for each array compared to its average value for all arrays, within a scale from twofold increase (yellow) to twofold decrease (blue). **d**, *p35* mRNA expression was quantified by RT–PCR in lymph nodes and spleen from naive C57BL/6 and B-cell-deficient JHT mice, as well as in B cells purified from lymph nodes and spleen of C57BL/6 mice. Data show compilation of three independent experiments (mean ± s.e.m.). **e**, Splenic B cells were activated as indicated for 72 h, and treated with GolgiStop for the last 4 h of culture. B-cell lysates were separated on SDS–PAGE gel and blotted with anti-EBI3 or anti-actin antibody. Data shows a representative result from three independent experiments. **f**, B cells from C57BL/6 or p35-deficient mice were activated for 72 h with LPS plus anti-CD40. Culture supernatants were subjected to immunoprecipitation with anti-p35 followed by western blot with anti-EBI3 antibody. Data shown are representative of two independent experiments.

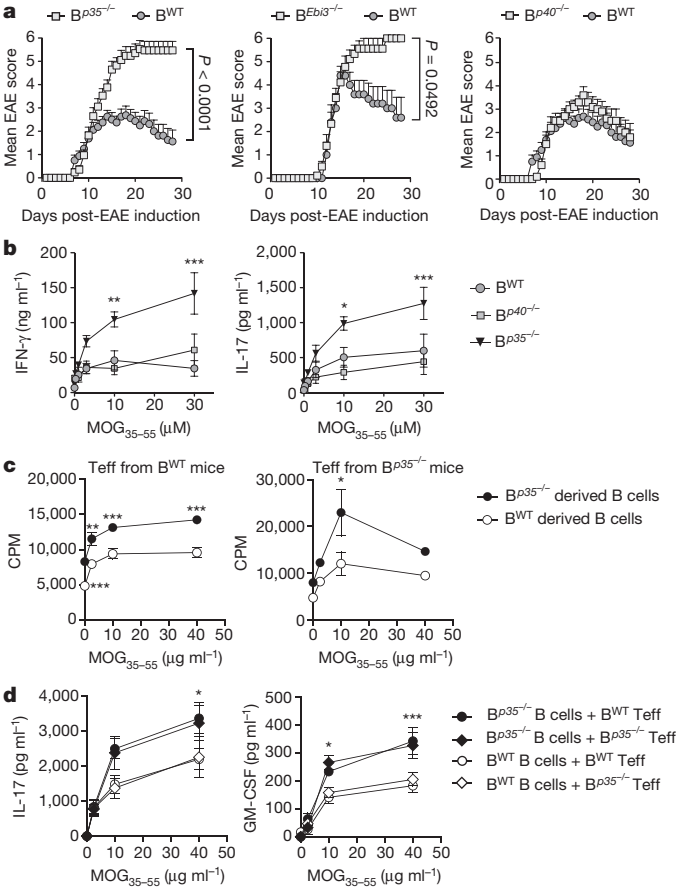

Figure 2 | IL-35 expression by B cells is required for recovery from EAE. **a**, EAE was induced in $B^{p35^{-/-}}$ (grey squares, $n = 17$) and B^{WT} mice (black circles, $n = 16$) (left panel); $B^{Ebi3^{-/-}}$ (grey squares, $n = 9$) and corresponding B^{WT} mice (black circles, $n = 5$) (middle panel); $B^{p40^{-/-}}$ (grey squares, $n = 10$) and B^{WT} mice (black circles, $n = 16$) (right panel) by immunization with $MOG_{35–55}$ peptide in Complete Freund's adjuvant. Data show clinical EAE scores from two independent experiments (mean ± s.e.m.). Cumulative disease scores were compared using a two-tailed unpaired *t*-test. **b**, Splenocytes were collected from mice on day 10 after EAE induction, and pooled before re-stimulation for 48 h with $MOG_{35–55}$ in increasing concentrations. Culture supernatants were analysed by ELISA to determine IFN-γ and IL-17 concentrations. Data show a representative result from two independent experiments. **c**, EAE was induced in $B^{p35^{-/-}}$ and corresponding B^{WT} mice by immunization with $MOG_{35–55}$ peptide in Complete Freund's adjuvant. B cells and CD4$^+$CD25$^-$ T cells (Teff) were isolated from pooled draining lymph nodes and spleens on day 10 after immunization. Then 5×10^5 B cells from $B^{p35^{-/-}}$ or B^{WT} mice were cultured with 1×10^4 Teff cells from $B^{p35^{-/-}}$ or B^{WT} mice in the presence of $MOG_{35–55}$ in increasing concentrations, as indicated. Proliferation was assessed after 64 h by [^{3}H]thymidine incorporation. CPM, counts per minute. Data show representative results from two independent experiments. **d**, Supernatants from cultures as described in **c** were harvested after 48 h, and analysed by Bio-Plex to determine the concentrations of IL-17 and GM-CSF. Data shown (mean ± s.e.m.) are pooled from two independent experiments. **b**–**d**, Graphs show mean ± s.e.m.. Results were compared using a two-way ANOVA followed by a Bonferroni post-test (*$P < 0.05$, **$P < 0.01$; ***$P < 0.001$). Results of comparison are shown for $B^{p35^{-/-}}$ versus B^{WT} (**b**), and for B^{WT} B cells plus B^{WT} Teff versus $B^{p35^{-/-}}$ B cells plus B^{WT} Teff (**d**).

to B^{WT} controls (Fig. 2a and Extended Data Fig. 2). Therefore, B cells limited EAE pathogenesis through provision of IL-35. EAE pathogenesis involves T_H1 and T_H17 cells, which express IFN-γ and IL-17, respectively[21,22]. $B^{p35^{-/-}}$ mice displayed increased MOG-reactive IFN-γ and IL-17 production compared to control mice (Fig. 2b and Extended Data Fig. 2d). In contrast, $B^{p28^{-/-}}$ and $B^{p40^{-/-}}$ mice mounted normal T-cell responses (Fig. 2b and Extended Data Fig. 2). $B^{p35^{-/-}}$ mice had more CD4$^+$ T cells and mononuclear phagocytes in the central nervous system than B^{WT} mice (Extended Data Fig. 2), suggesting that B-cell-derived IL-35 limited disease by reducing the accumulation of pathogenic cells in the target organ. These data demonstrate that B-cell-derived IL-35 is a critical regulator of T-cell-mediated autoimmunity.

The mechanisms underlying the suppressive activities of IL-35 remain poorly understood[23]. During EAE, the increased T-cell response observed in $B^{p35^{-/-}}$ mice was not due to a defect in CD4$^+$Foxp3$^+$ T regulatory (Treg) cells (Extended Data Fig. 2), which are protective in this disease[24]. B cells from $B^{p35^{-/-}}$ mice expressed higher levels of activation markers (CD44, CD69) and molecules involved in antigen presentation to CD4$^+$ T cells (MHC-II, CD80, CD86), compared to control B cells (Extended Data Fig. 3). Accordingly, they were more potent APC, stimulating higher proliferation and production of inflammatory cytokines (IL-17 and GM-CSF) by MOG-reactive CD4$^+$ T cells than control B cells (Fig. 2c, d and Extended Data Fig. 3c). Preliminary studies showed that $B^{p35^{-/-}}$ mice were susceptible to EAE induced with human MOG, a

disease dependent on pathogenic functions of B cells[25]. These findings introduce IL-35 as a regulator of the APC function of B cells.

To test the role of B-cell-derived IL-35 in infection, we challenged $B^{p35^{-/-}}$, $B^{Ebi3^{-/-}}$ and $B^{p40^{-/-}}$ mice with the Gram-negative bacterium *Salmonella enterica* serovar Typhimurium (hereafter referred to as *Salmonella*). This intracellular pathogen causes a disease in mice that resembles typhoid fever in humans, responsible for approximately 20 million cases and 600,000 deaths annually[26]. $B^{p35^{-/-}}$ and $B^{Ebi3^{-/-}}$ mice displayed longer survival than $B^{p40^{-/-}}$ and B^{WT} mice after primary infection, and upon secondary challenge (Fig. 3a). This improved resistance correlated with better control of the bacterial burden in spleen and liver, increased accumulation of macrophages in these organs, and stronger inflammatory T-cell responses towards *Salmonella* (Fig. 3b, c and Extended Data Fig. 4). In contrast, B-cell-derived IL-35 had no effect on Treg frequencies, global frequencies of activated T cells or humoral immunity against *Salmonella* (Extended Data Figs 4 and 5a). $B^{p35^{-/-}}$ mice also mounted normal antibody responses against a hapten-protein antigen (Extended Data Fig. 5b). Consistent with the role of CD40 in IL-35 production by B cells (Fig. 1), mice with a B-cell-restricted deficiency in CD40 displayed enhanced control of *Salmonella* infection (Extended Data Fig. 5c). These data demonstrate that B cells can inhibit anti-microbial immunity through production of IL-35.

B cells can also inhibit anti-*Salmonella* immunity through IL-10 (ref. 6). To identify IL-10- and IL-35-producing B cells, and clarify their relationship, we quantified *Ebi3* and *Il10* mRNA in $CD19^+CD138^-$ B cells and $CD138^{hi}$ plasma cells during *Salmonella* infection (Fig. 4a and Extended Data Fig. 6). *Ebi3* and *Il10* were exclusively induced in $CD138^{hi}$ cells (Fig. 4a). Single-cell PCR analyses indicated that distinct sets of $CD138^{hi}$ cells expressed the mRNA for *Il10* or for both IL-35 subunits *Ebi3* and *p35* (Fig. 4b). We therefore characterized further these plasma cells. They expressed uniform surface levels of IgM, CD80, CD86, MHC-II, CD40, CD69, CD44, CD43, TACI and CXCR4, as well as intermediate levels of CD1d (also known as Cd1d1) and Tim1 (also known as Havcr1) (Extended Data Fig. 6a, d), yet three subsets could be distinguished according to CD138 and CD22 levels: $CD138^{int}CD22^+$, $CD138^{hi}CD22^+$ and $CD138^{hi}CD22^-$ cells (Extended Data Fig. 7). These subsets differed by their capacity to produce antibodies, and expressed distinct amounts of mRNA for the transcription factors driving plasma cell development (Blimp1, IRF4), or maintaining B-cell identity (Pax5) (Extended Data Fig. 7), demonstrating that they corresponded to different stages of plasma cell development. The expression levels of *Il10* and *Ebi3* mRNA in these subsets correlated with their degree of maturity, and were highest in the most differentiated $CD138^{hi}CD22^-$ cells (Extended Data Fig. 7c). $CD138^{hi}CD22^-$ plasma cells were mostly located at the interface between red and white pulp in spleen, in clusters also containing T cells, $CD11b^+$ and $CD169^+$ myeloid cells (Extended Data Fig. 7d). Single-cell PCR analyses revealed that 6–10% of $CD138^{hi}$ cells expressed *Il10* mRNA, and a similar frequency made mRNA for both IL-35 subunits, whereas few cells co-expressed these three transcripts together (Fig. 4b). Nearly all $CD138^{hi}$ cells transcribing *Il10* or both IL-35 subunits co-expressed *Blimp1* (Fig. 4c), as expected for plasma cells. The less mature $CD138^{int}CD22^+$ population contained little *Il10* or *Ebi3* mRNA (Extended Data Fig. 7c), and only rare cells contained *Il10* mRNA (Fig. 4b), suggesting that expression of IL-10 and both IL-35 subunits were acquired during plasma cell maturation. These data indicate that distinct sets of plasma cells provide IL-10 and IL-35 during *Salmonella* infection.

Plasma cells from mice infected with *Salmonella* consistently secreted more IL-10 than B cells upon *ex vivo* stimulation (Fig. 4d and Extended Data Fig. 8). Around 70% of $CD138^{hi}$ plasma cells upregulated IL-10 expression after stimulation with phorbol 12-myristate 13-acetate plus ionomycin, a classical treatment for identifying cytokine-producing cells (Extended Data Fig. 8). $CD138^+$ plasma cells were also the major B-cell subtype expressing the proteins EBI3 and p35 (Fig. 4e). In contrast, $CD138^{hi}$ plasma cells did not secrete IL-6, a mediator of pro-inflammatory functions of B cells[27], unlike $CD19^+CD138^-$ B cells (Extended Data Fig. 8). This lack of IL-6 production, which may reflect a repressive effect of Blimp1 (ref. 28), distinguishes IL-10- and IL-35-expressing plasma cells from IL-10-producing $CD1d^{hi}$ B cells (Extended Data Fig. 8). $CD138^{hi}$ plasma cells therefore have a remarkable propensity to express anti-inflammatory cytokines but not IL-6 during *Salmonella*

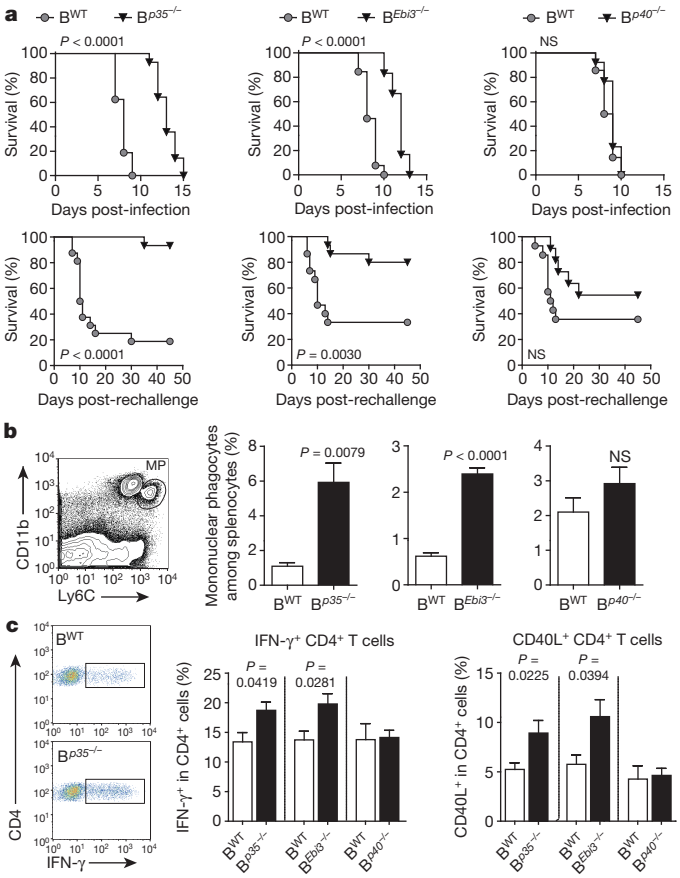

Figure 3 | B-cell-derived IL-35 enhances susceptibility to *Salmonella*. **a**, Top panel shows survival curves of $B^{p35^{-/-}}$ ($n = 14$) and corresponding B^{WT} mice ($n = 16$), $B^{Ebi3^{-/-}}$ ($n = 12$) and corresponding B^{WT} mice ($n = 13$), $B^{p40^{-/-}}$ ($n = 13$) and corresponding B^{WT} mice ($n = 14$) after infection with virulent *Salmonella* (SL1344). Data pooled from two independent experiments. Survival curves were compared using Wilcoxon test. Bottom panel shows survival curves of $B^{p35^{-/-}}$ ($n = 15$) and corresponding B^{WT} mice ($n = 16$), $B^{Ebi3^{-/-}}$ ($n = 15$) and corresponding B^{WT} mice ($n = 15$), $B^{p40^{-/-}}$ ($n = 11$) and corresponding B^{WT} mice ($n = 14$) vaccinated with attenuated *Salmonella* (SL7207) and 90 days later re-challenged with virulent *Salmonella* (SL1344). Data are pooled from two independent experiments. Survival curves were compared using Wilcoxon test. **b**, Representative FACS plot of mononuclear phagocytes (MP) gated as $CD11b^+Ly6C^{hi}$ cells among live B^{WT} splenocytes at day 6 post-infection (p.i). with SL1344 (left panel); frequencies of MP per spleen at day 6 p.i. in $B^{p35^{-/-}}$, $B^{Ebi3^{-/-}}$, and $B^{p40^{-/-}}$ mice together with their corresponding B^{WT} controls (right panel). Numbers of mice: $B^{p35^{-/-}}$ ($n = 6$) and B^{WT} ($n = 8$), $B^{Ebi3^{-/-}}$ ($n = 7$) and B^{WT} ($n = 5$), $B^{p40^{-/-}}$ ($n = 8$) and B^{WT} ($n = 8$). Data are pooled from two independent experiments. Graphs show mean ± s.e.m. **c**, Mice were infected with attenuated *Salmonella* (SL7207). After 21 days, bone marrow cells were stained for CD4 and CD40L or IFN-γ after 6 h re-stimulation with heat-killed *Salmonella*. Representative FACS plots of IFN-γ^+ cells among $CD4^+$ T cells from B^{WT} and $B^{p35^{-/-}}$ mice (left panel). Frequencies of IFN-γ^+ and $CD40L^+$ cells among $CD4^+$ T cells, (middle and right panels, respectively). Data are pooled from two independent experiments with total number of mice: $B^{p35^{-/-}}$ ($n = 12$) and corresponding B^{WT} ($n = 10$), $B^{Ebi3^{-/-}}$ ($n = 8$) and corresponding B^{WT} ($n = 9$), $B^{p40^{-/-}}$ ($n = 15$) and corresponding B^{WT} ($n = 9$). **b**, **c**, Data were analysed using two-tailed unpaired *t*-test with Welch's correction in case of unequal variance. *P* values >0.05 are considered not significant (NS).

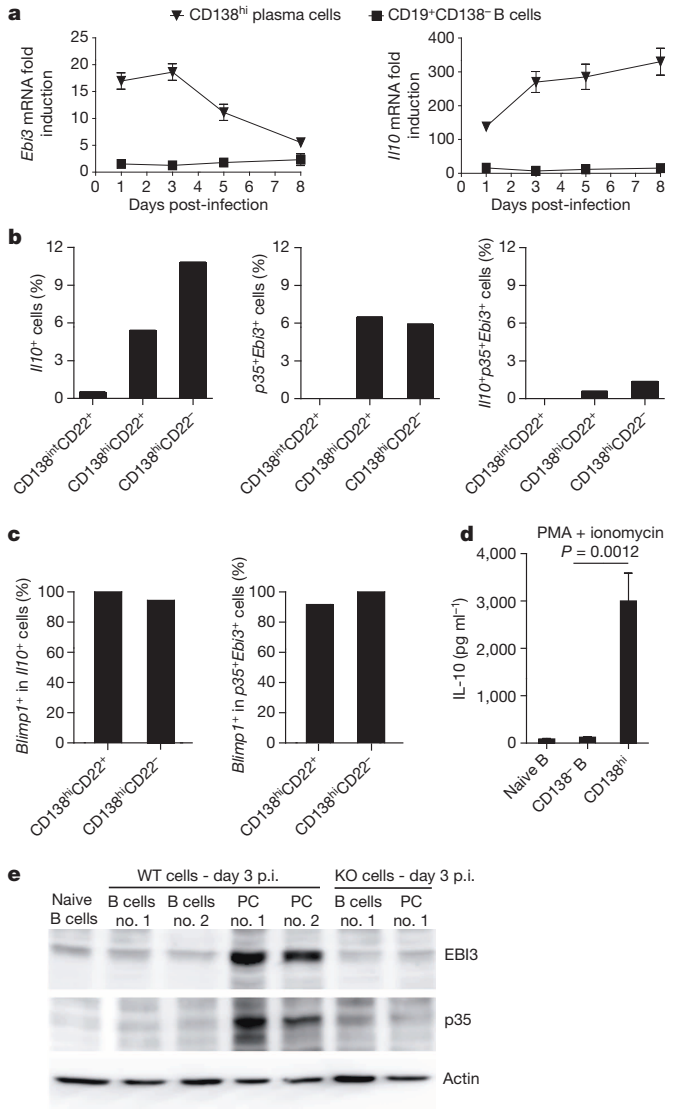

Figure 4 | IL-10 and IL-35 are expressed by CD138^{hi} plasma cells during *Salmonella* infection. **a**, Splenic plasma cells (PC) (CD138^{hi}) and B cells (CD19^{+}CD138^{-}) were isolated from C57BL/6 mice on days 0, 1, 3, 5, and 8 after infection with 10^7 c.f.u. attenuated *Salmonella* (SL7207). *Ebi3* and *Il10* mRNA expression was quantified by RT–PCR. Data show fold induction of *Ebi3* (left) and *Il10* (right) in PC and B cells compared to naive B cells. A compilation of five independent experiments is shown (mean ± s.e.m.). **b**, Single CD138^{int}CD22^{+}, CD138^{hi}CD22^{+}, and CD138^{hi}CD22^{-} cells were sorted by FACS from C57BL/6 mice on day 3 after infection with 10^7 c.f.u. attenuated *Salmonella* (SL7207). A total of 208 CD138^{int}CD22^{+}, 206 CD138^{hi}CD22^{+} and 189 CD138^{+}CD22^{-} cells expressed β-actin, and were included for analysis. Data show percentages of *Il10*$^{+}$ (left), *p35*$^{+}$*Ebi3*$^{+}$ (middle), and *Il10*$^{+}$*p35*$^{+}$*Ebi3*$^{+}$ (right) cells among each subset. **c**, *Blimp1* mRNA expression in cells analysed in (**c**) was also detected by single-cell PCR. Data show percentages of *Blimp1*$^{+}$ cells among *Il10*$^{+}$ (left), and *p35*$^{+}$*Ebi3*$^{+}$ cells (right). **d**, CD138^{hi} PC and CD19^{+}CD138^{-} B cells were isolated from spleens of C57BL/6 mice on day 3 after infection with attenuated *Salmonella* (10^7 c.f.u.). Naive B splenic B cells were isolated from unchallenged C57BL/6 mice. Cells were activated for 24 h with PMA/ionomycin and IL-10 was determined in culture supernatants by Bio-Plex. Data shown is pooled from 5 independent experiments. Results were compared using a two-tailed unpaired *t*-test. **e**, Splenic CD19^{+}CD138^{-} B cells and CD138^{+} plasma cells were isolated from spleens of C57BL/6 (WT) and *p35*$^{-/-}$*Ebi3*$^{-/-}$*p40*$^{-/-}$ mice on day 3 p.i. with attenuated *Salmonella* (10^7 c.f.u.). Proteins were separated on SDS–PAGE gel and detected with anti-EBI3, anti-p35 or anti-actin antibodies. Data show results from two independent preparations for WT samples, and one preparation for *p35*$^{-/-}$*Ebi3*$^{-/-}$*p40*$^{-/-}$ B and plasma cells.

infection, emphasizing the regulatory potential of plasma cells compared to other B cell subsets.

Our study identifies IL-35-producing B cells as critical regulators of immunity. At a time window during *Salmonella* infection when both B-cell-derived IL-10 (ref. 6) and IL-35 exerted suppressive functions, plasma cells were the major B-cell type expressing these cytokines. This was also the case during EAE (Extended Data Fig. 9). During *Salmonella* infection, IL-10 and IL-35 were made by distinct sets of plasma cells, suggesting that these two suppressive axes can operate in parallel. In line with this, mice in which individual B cells could express either IL-10 or IL-35, but not both cytokines, displayed a normal EAE course (Extended Data Fig. 9). Accordingly, B and plasma cells could produce IL-10 without concomitant IL-35 secretion (Extended Data Fig. 9). Future studies shall assess whether 'regulatory plasma cells' producing IL-10 and IL-35 (but not IL-6) can provide novel opportunities for immune intervention.

METHODS SUMMARY

B$^{Tlr2-/-}$, B$^{Tlr4-/-}$, B$^{p35-/-}$, B$^{Ebi3-/-}$, B$^{p40-/-}$, B$^{p28-/-}$ and B^{WT} mice were generated using a previously described mixed bone marrow chimaera approach[3,6], as detailed in the Methods, and outlined in Extended Data Fig. 10. This protocol allowed normal reconstitution of the B-cell compartment in the resulting chimaera (Extended Data Fig. 10). EAE was induced in mice by immunization with MOG_{35-55} emulsified in complete Freund's adjuvant (Sigma-Aldrich). The disease score and the MOG_{35-55} specific T-cell responses (at days 10 and 28) were assessed as described previously[3]. Mouse B cells were purified and activated as described before[15]. Cytokine secretion was determined by Bio-Plex or ELISA. Whole transcriptome analyses were performed with RNA purified from naive and activated B cells, using GeneChip Mouse Genome 430 2.0 Arrays. For mRNA quantification, total RNA was isolated with TRIzol (AMS Biotechnology) and cDNA was prepared with the Reverse Transcription Kit (Promega). Quantitative RT–PCR was performed with LightCycler FastStart DNA Master SYBR Green I (Roche). Western blots to determine EBI3, p35 and actin expression were performed using anti-EBI3 (rabbit M75 polyclonal Ab), anti-p35 (rabbit EPR5736 polyclonal Ab), and anti-actin (rabbit I-19 polyclonal Ab), respectively. For immunoprecipitation, IL-35 was captured with anti-p35 antibody (clone C18.2; eBioscience) followed by precipitation using μMACS Protein G microbeads (Miltenyi Biotech). Infections with virulent and attenuated *Salmonella* (strains SL1344 and SL7207, respectively) were performed as published[6]. Flow cytometry analyses were performed as previously described[6]. Other protocols are described in the Methods.

Online Content Any additional Methods, Extended Data display items and Source Data are available in the online version of the paper; references unique to these sections appear only in the online paper.

Received 24 January 2012; accepted 30 December 2013.
Published online 23 February 2014.

1. Fillatreau, S., Gray, D. & Anderton, S. M. Not always the bad guys: B cells as regulators of autoimmune pathology. *Nature Rev. Immunol.* **8,** 391–397 (2008).
2. Fillatreau, S. Novel regulatory functions for Toll-like receptor-activated B cells during intracellular bacterial infection. *Immunol. Rev.* **240,** 52–71 (2011).
3. Fillatreau, S., Sweenie, C. H., McGeachy, M. J., Gray, D. & Anderton, S. M. B cells regulate autoimmunity by provision of IL-10. *Nature Immunol.* **3,** 944–950 (2002).
4. Mauri, C., Gray, D., Mushtaq, N. & Londei, M. Prevention of arthritis by interleukin 10-producing B cells. *J. Exp. Med.* **197,** 489–501 (2003).
5. Mizoguchi, A., Mizoguchi, E., Takedatsu, H., Blumberg, R. S. & Bhan, A. K. Chronic intestinal inflammatory condition generates IL-10-producing regulatory B cell subset characterized by CD1d upregulation. *Immunity* **16,** 219–230 (2002).
6. Neves, P. *et al.* Signaling via the MyD88 adaptor protein in B cells suppresses protective immunity during *Salmonella typhimurium* infection. *Immunity* **33,** 777–790 (2010).
7. Duddy, M. *et al.* Distinct effector cytokine profiles of memory and naive human B cell subsets and implication in multiple sclerosis. *J. Immunol.* **178,** 6092–6099 (2007).
8. Jagannathan, M. *et al.* Toll-like receptors regulate B cell cytokine production in patients with diabetes. *Diabetologia* **53,** 1461–1471 (2010).
9. Benedetti, L. *et al.* Relapses after treatment with rituximab in a patient with multiple sclerosis and anti myelin-associated glycoprotein polyneuropathy. *Arch. Neurol.* **64,** 1531–1533 (2007).
10. Goetz, M., Atreya, R., Ghalibafian, M., Galle, P. R. & Neurath, M. F. Exacerbation of ulcerative colitis after rituximab salvage therapy. *Inflamm. Bowel Dis.* **13,** 1365–1368 (2007).
11. El Fassi, D., Nielsen, C. H., Kjeldsen, J., Clemmensen, O. & Hegedus, L. Ulcerative colitis following B lymphocyte depletion with rituximab in a patient with Graves' disease. *Gut* **57,** 714–715 (2008).

12. Dass, S., Vital, E. M. & Emery, P. Development of psoriasis after B cell depletion with rituximab. *Arthritis Rheum.* **56,** 2715–2718 (2007).
13. Wilson, M. S. *et al.* Helminth-induced $CD19^{+}CD23^{hi}$ B cells modulate experimental allergic and autoimmune inflammation. *Eur. J. Immunol.* **40,** 1682–1696 (2010).
14. Su, Y., Zhang, A. H., Noben-Trauth, N. & Scott, D. W. B-cell gene therapy for tolerance induction: host but not donor B-cell derived IL-10 is necessary for tolerance. *Front. Microbiology* **2**, http://dx.doi.org/10.3389/fmicb.2011.00154 (2011).
15. Lampropoulou, V. *et al.* TLR-activated B cells suppress T cell-mediated autoimmunity. *J. Immunol.* **180,** 4763–4773 (2008).
16. Devergne, O., Birkenbach, M. & Kieff, E. Epstein-Barr virus-induced gene 3 and the p35 subunit of interleukin 12 form a novel heterodimeric hematopoietin. *Proc. Natl Acad. Sci. USA* **94,** 12041–12046 (1997).
17. Collison, L. W. *et al.* The inhibitory cytokine IL-35 contributes to regulatory T-cell function. *Nature* **450,** 566–569 (2007).
18. Niedbala, W. *et al.* IL-35 is a novel cytokine with therapeutic effects against collagen-induced arthritis through the expansion of regulatory T cells and suppression of Th17 cells. *Eur. J. Immunol.* **37,** 3021–3029 (2007).
19. Villarino, A. *et al.* The IL-27R (WSX-1) is required to suppress T cell hyperactivity during infection. *Immunity* **19,** 645–655 (2003).
20. Brentano, F. *et al.* Abundant expression of the interleukin (IL)23 subunit p19, but low levels of bioactive IL23 in the rheumatoid synovium: differential expression and Toll-like receptor-(TLR) dependent regulation of the IL23 subunits, p19 and p40, in rheumatoid arthritis. *Ann. Rheum. Dis.* **68,** 143–150 (2009).
21. Kuchroo, V. K. *et al.* Cytokines and adhesion molecules contribute to the ability of myelin proteolipid protein-specific T cell clones to mediate experimental allergic encephalomyelitis. *J. Immunol.* **151,** 4371–4382 (1993).
22. Park, H. *et al.* A distinct lineage of CD4 T cells regulates tissue inflammation by producing interleukin 17. *Nature Immunol.* **6,** 1133–1141 (2005).
23. Bettini, M., Castellaw, A. H., Lennon, G. P., Burton, A. R. & Vignali, D. A. Prevention of autoimmune diabetes by ectopic pancreatic β-cell expression of interleukin-35. *Diabetes* **61,** 1519–1526 (2012).
24. McGeachy, M. J., Stephens, L. A. & Anderton, S. M. Natural recovery and protection from autoimmune encephalomyelitis: contribution of $CD4^{+}CD25^{+}$ regulatory cells within the central nervous system. *J. Immunol.* **175,** 3025–3032 (2005).
25. Weber, M. S. *et al.* B-cell activation influences T-cell polarization and outcome of anti-CD20 B-cell depletion in central nervous system autoimmunity. *Ann. Neurol.* **68,** 369–383 (2010).
26. Mittrücker, H. W. & Kaufmann, S. H. Immune response to infection with *Salmonella typhimurium* in mice. *J. Leukoc. Biol.* **67,** 457–463 (2000).
27. Barr, T. A. *et al.* B cell depletion therapy ameliorates autoimmune disease through ablation of IL-6-producing B cells. *J. Exp. Med.* **209,** 1001–1010 (2012).
28. Chan, Y. H. *et al.* Absence of the transcriptional repressor Blimp-1 in hematopoietic lineages reveals its role in dendritic cell homeostatic development and function. *J. Immunol.* **183,** 7039–7046 (2009).

Acknowledgements We thank H. Schliemann, H. Ruebsamen, M. Spadaro and D. Jenne for assistance and support. We thank M. Loehning for providing IL-12 p40-deficient mice, and S. Akira for providing TLR2- and TLR4-deficient mice. We thank O. Neyrolles for help with some of the *in vivo* experiments. We thank E. Schott for help with the AST/ALT measurements. S.F. is supported by grants from the Deutsche Forschungsgemeinschaft (SFB-650, TRR-36, TRR-130, FI-1238/02), Hertie Stiftung, and an advanced grant from the Merieux Institute. C.D and T.D. are supported by the Deutsche Forschungsgemeinschaft (SFB-650, Do491/7-2, 8-2). P.B. and L.J. are supported by INRA. A.B.-O. is supported by a CIHR/MSSC New Emerging Team grant in Clinical Autoimmunity. Work in S.M.A.'s laboratory was supported by grants from the UK Medical Research Council and the Wellcome Trust. E.M. is supported by the Clinical Competence Network for Multiple Sclerosis and SFB-TR128.

Author Contributions P.S., T.R. and V.L. performed most of the experiments, the data analysis, and edited the manuscript. R.A.O., U.S., E.H., S.R., V.D.D., Y.J., C.D., R.L., L.J., P.B., S.W., I.S., Y.M., M.D.L., R.C.M., S.W., M.N., K.H., E.M., A.G., J.R.G., K.H., A.A.K., T.D., A.B.-O., S.H.E.K. and S.M.A. contributed to some experiments. L.J., P.B., A.G. and J.R.G. performed the microarray data analysis. T.D., S.H.E.K. and S.M.A. helped with the writing of the manuscript. S.M.A. helped with the design of some experiments. S.F. designed the study, performed some experiments and wrote the manuscript.

Author Information The gene array data have been deposited in NCBI's Gene Expression Omnibus database with the accession number GSE35998. Reprints and permissions information is available at www.nature.com/reprints. The authors declare no competing financial interests. Readers are welcome to comment on the online version of the paper. Correspondence and requests for materials should be addressed to S.F. (fillatreau@drfz.de).

METHODS

Mice, immunization and infection. C57BL/6, *Tlr2*$^{-/-}$, *Tlr4*$^{-/-}$, *Ebi3*$^{-/-}$, *p28*$^{-/-}$, *p35*$^{-/-}$, *p40*$^{-/-}$, *Cd40*$^{-/-}$, *Il10*$^{-/-}$, *Il10*$^{-/-}$*p35*$^{-/-}$, *p35*$^{-/-}$*Ebi3*$^{-/-}$p40$^{-/-}$, JHT, IL-10–eGFP[6], and *p35*$^{-/-}$ IL10–eGFP mice were bred under specific pathogen-free conditions. B$^{Tlr2^{-/-}}$, B$^{Tlr4^{-/-}}$, B$^{p28^{-/-}}$, B$^{p35^{-/-}}$, B$^{Ebi3^{-/-}}$, B$^{p40^{-/-}}$, B$^{Cd40^{-/-}}$ and B$^{Il10^{-/-}}$ mice were obtained by a previously described mixed bone marrow chimaera approach using lethally irradiated C57BL/6 or JHT mice as recipients[3,6]. Briefly, B$^{p35^{-/-}}$ mice were obtained by reconstituting recipient mice with a mixture of bone marrow cells from B-cell-deficient JHT mice (80%) and p35-deficient mice (20%). Control B^{WT} chimaera were obtained using a mixture of bone marrow cells from JHT mice (80%) and C57BL/6 mice (20%) for experiments shown in Fig. 1a, Fig. 2a left panel, and Fig. 2a, right panel. For all other experiments (including Fig. 2a middle panel, and Extended Data Fig. 2a), corresponding B^{WT} control chimaera were obtained as outlined in Extended Data Fig. 10, by reconstituting irradiated mice with a mixture of bone marrow cells from C57BL/6 mice (80%) and from mice deficient in the gene of interest (20%). The various control chimaera are called 'corresponding B^{WT} mice' throughout the study. EAE was induced by immunization with MOG_{35-55} peptide, or recombinant human MOG extracellular domain emulsified in Complete Freund's adjuvant (Sigma-Aldrich) and pertussis toxin (Sigma-Aldrich), and assessed as previously described[3]. Mice with a weight loss >20% were humanely euthanized according to ethical regulations. To measure the MOG-reactive T cell response, 8×10^5 splenocytes were stimulated in flat-bottomed 96-well plates with different concentrations of MOG_{35-55} peptide for 2 days, and culture supernatants were then analysed by ELISA to determine concentrations of IFN-γ and IL-17 (coating/detection with clones R4-6A2 and XMG1.2 for IFN-γ, and TC11-18H10 and TC11-8H4 for IL-17). Mice were infected intravenously with 100 c.f.u. *Salmonella* strain SL1344, and 10^6 or 10^7 c.f.u. attenuated *Salmonella* strain SL7207, and assessed as previously described, including for histological analyses[6]. All experiments were reviewed and approved by appropriate institutional review committees (University of Edinburgh ethical review committee, Comite d'Ethique Midi-Pyrenees, and LAGeSo Berlin), and were conducted in accordance with UK, French and German legislations, in compliance with European community council directive 68/609/EEC guidelines. Mice were of C57BL/6 strain, 6–12-weeks old at the start of experiments, and of male and female genders. EAE experiments and *Salmonella* infections were performed in a blinded manner, and identities of the mice were revealed upon termination of the experiment. No randomization was used. Estimation of size groups was based on our previous experience with these disease models, without a priori determination by power calculation.

B-cell purification and activation. B cells were obtained by magnetic isolation using negative selection with anti-CD11b, anti-CD11c, and anti-CD43 microbeads (Miltenyi Biotec). B cells (>99% pure) were activated as previously described[15] at 5×10^5 cells per well in 96-well flat-bottom plates with LPS (*Escherichia coli* serotype 055:B5; Sigma-Aldrich), CpG-ODN-1826 (TIB MolBiol, Germany), PGN (*Streptomyces* species 79682; Sigma-Aldrich), agonistic anti-CD40 antibody (clone FGK-45, produced in house), mouse CD40L-expressing L47 cells (L47-CD40L$^+$), or control L5 cells (L5-ctrl) as indicated. Culture supernatants were collected at 72 h, and IL-10 concentrations measured by Bio-Plex (Bio-Rad). For the microarray experiments, B cells purified as described above were further depleted of possible contaminants by another round of magnetic negative selection after relabelling with anti-CD11b, anti-CD11c, anti-CD43, anti-CD90, and anti-DX5 microbeads (Miltenyi Biotec). B cells were activated with LPS (1 μg ml^{-1}) or LPS (1 μg ml^{-1}) plus anti-CD40 (10 μg ml^{-1}). Dead cells were eliminated from the 24 h and 72 h activated culture by labelling with propidium iodide (PI), and sorting on FACS Diva (BD Biosciences). Cells were lysed in RLT buffer (Qiagen) and total RNA was extracted using RNeasy Mini Kit (Qiagen).

Gene array hybridization and data analysis. cRNA were hybridized on Affymetrix MG 430 2.0 arrays, using standard Affymetrix protocol after quality control with Agilent 2100 Bioanalyzer and quantification with NanoDrop ND-1000 spectrophotometer, as previously described[29]. The significantly differentially regulated genes were detected using a *t*-test based R-script, with *P* values adjusted using Benjamini Hochberg procedure. In order to be selected in a comparison of two conditions, each Affymetrix ID had to fulfill the following criteria: (1) be present in at least three of the four arrays for at least one of the two conditions compared, (2) to have a mean signal intensity higher than 50 in at least one of the two conditions, and (3) to show an adjusted *P* value <0.01 (*t*-test) in the comparison of the two conditions. The genes differentially expressed between TLR4-activated and TLR4-activated plus CD40-activated B cells (*t*-test; $P < 0.01$), and differentially modulated during B-cell activation (*t*-test; $P < 0.01$), were then selected and filtered using the gene ontology resource (http://www.geneontology.org) to focus on secreted molecules (Extended Data Fig. 1c). Seven genes fulfilled these criteria, among which five were uniquely increased in TLR4 plus CD40-stimulated B cells (Extended Data Fig. 1c). Hierarchical clustering was performed with the MeV program (version 4.8.1)[30] using Pearson correlation and average linkage.

Analysis of mRNA expression by B and plasma cells. Sorted B and plasma cells were lysed in TRIzol, and RNA was prepared (AMS Biotechnology). After DNase treatment (Ambion), RNA was reverse-transcribed with a Reverse Transcription System (Promega). Quantitative RT–PCR was performed on an MX3005P QPCR System (Stratagene), with LightCycler FastStart DNA Master SYBR Green I (Roche). Transcripts were quantified using β-actin as standard, and the following forward (FP) and reverse (RP) primers (MWG Biotech): β-actin FP: 5′-TGGAATCCTG TGGCATCCATGAAAC-3′, β-actin RP: 5′-TAAAACGCAGCTCAGTAACAG TCC-3′; EBI3 FP: 5′-CGGTGCCCTACATGCTAAAT-3′, EBI3 RP: 5′-GCGGAG TCGGTACTTGAGAG-3′; p35 FP: 5′- CATCGATGAGCTGATGCAGT-3′, p35 RP: 5′-CAGATAGCCCATCACCCTGT-3′; IL-10 FP: 5′-AGCCGGGAAGAC AATAACTG-3′, IL-10 RP: 5′-CATTTCCGATAAGGCTTGG-3′; Blimp1 FP: 5′- GGCATTCTTGGGAACTGTGT-3′; Blimp1 RP: 5′- GACAGAGGCCGAGT TTGAAG-3′; IRF4 FP: 5′- GCAGCTCACTTTGGATGACA-3′; IRF4 RP: 5′-CC AAACGTCACAGGACATTG-3′; Pax5 FP: 5′-AACTTGCCCATCAAGGTGTC-3′; Pax5 RP: 5′-CTGATCTCCCAGGCAAACAT-3′.

Western blot and immunoprecipitation. Activated B cells were treated with GolgiStop (BD Biosciences, Germany) to block protein secretion during the last 4 h of stimulation. B cells (2×10^7) were lysed with 500 μl RIPA buffer (Thermo Fisher Scientific, USA) supplemented with protease inhibitors (Thermo Fisher Scientific, USA). Cells isolated from mice infected with *Salmonella* were directly lysed in RIPA buffer containing protease inhibitors. Protein concentrations of lysates were determined using the BCA Protein Assay Kit (Thermo Fisher Scientific, USA). Proteins were separated on a polyacrylamide gel and transferred to a PVDF membrane (Bio-Rad Laboratories, USA) using semi-dry blotting. EBI3, p35 and actin were detected using rabbit anti-EBI3 (M-75 polyclonal IgG, Santa Cruz Biotechnology, USA), rabbit anti-p35 (EPR5736 polyclonal IgG, Abcam, UK), or rabbit anti-actin (I-19 polyclonal Ab, Santa Cruz Biotechnology, USA) primary antibody, and horseradish peroxidase (HRP)-conjugated secondary anti-rabbit antibody (cat. number: 81-6120, Invitrogen, USA; or cat. number: 111-035-144, Jackson ImmunoResearch, USA) with ECL (GE Healthcare, UK) as HRP substrate. The chemiluminescence signal was measured using the Image-Reader LAS-3000 (Fujifilm, Japan). For immunoprecipitation, supernatant from B cells activated with LPS plus anti-CD40 (clone FGK-45, 10 μg ml^{-1}) were incubated overnight at 4 °C with 2 μg ml^{-1} anti-p35 (C18.2, eBioscience). Immunoprecipitation was performed using μMACS Protein G Microbeads (Miltenyi Biotech), followed by immunoblot to detect EBI3.

B–T cell co-cultures. The protocol for B–T cell co-cultures was adapted from a previous report[25]. Briefly, B cells were magnetically sorted from pooled spleens and lymph nodes of B$^{p35^{-/-}}$ or B^{WT} mice on day 10 post-EAE induction as CD19$^+$ cells (~98% pure), and Teff cells were FACS-sorted from the CD19-depleted fraction as previously described[31]. 50×10^4 B cells and 1×10^4 CD4$^+$CD25$^-$ T cells (Teff) were then co-cultured in the indicated combinations in presence of increasing concentrations of MOG_{35-55}. After 48 h cultures received 1 μCi [^{3}H]thymidine, and [^{3}H]thymidine incorporation was measured 16 h later with a Top-Count NXT liquid scintillation counter (Perkin Elmer). Before addition of [^{3}H]thymidine, samples of culture supernatants were collected to quantify concentrations of IL-17, IFN-γ, GM-CSF and IL-6 using Bio-Plex (Bio-Rad).

Plasma cell purification. Plasma cells and B cells were obtained from C57BL/6, *p35*$^{-/-}$, *p35*$^{-/-}$*Ebi3*$^{-/-}$*p40*$^{-/-}$, IL-10–eGFP, and p35$^{-/-}$IL-10–eGFP mice on day 3 after infection with 10^7 colony forming units (c.f.u.) *Salmonella* (SL7207) by magnetic isolation using anti-CD138-PE (clone 281-2, BD Pharmingen) and anti-PE microbeads (Miltenyi Biotec). The negative fraction was then subjected to FACS sorting to obtain high purity CD19$^+$CD138$^-$ B cells. The positive fraction was then stained for CD22 (clone OX-97, BioLegend), and subjected to FACS sorting to obtain high purity plasma cells (CD138^{hi}), and plasma cell subsets (CD138^{int}CD22$^+$, CD138^{hi}CD22$^+$ and CD138^{hi}CD22$^-$ cells). For western blot, CD138^{hi} and CD138^{int} cells were isolated as CD138$^+$ plasma cells from infected mice by magnetic isolation using anti-CD138-PE (clone 281-2, BD Pharmingen) and anti-PE microbeads (Miltenyi Biotec).

Single-cell PCR analysis. Single cells were sorted on a FACS Aria II (BD Biosciences) into a 96-well PCR plate, immediately frozen in liquid nitrogen and stored at −80 °C until further use. For detection of respective transcripts a two-step PCR approach was used. Reverse transcription and the first PCR step were carried out in a one-step reaction using the Qiagen OneStep RT–PCR kit according to the manufacturer's instructions. As recommended in these instructions, specific nested primers (MWG Biotech) were used as follows: EBI3nested FP: 5′-CCTTCATT GCCACTTACAGG-3′, EBI3nested RP: 5′-TAATCTGTGAGGTCCTGAGC-3′; p35nested FP: 5′-CATTCTAGACAAGGGCATGC-3′, p35nested RP: 5′-GTGAT GGGAGAACAGATTCC-3′; IL-10nested FP: 5′-TCTTACTGACTGGCATGAG G-3′; IL-10nested RP: 5′-CTTCTACCAGGTAAAACTGG-3′; Blimp1nested FP:

5′- CGTGAAGTTTCAAGGACTGG-3′; Blimp1nested RP: 5′- GTGGTGGAAC TCCTCTCTGG-3′. For validation of sorting, β-actin primers were added to the reaction mixture. After this first reaction, an aliquot of the PCR product was loaded on an agarose gel, and only β-actin positive samples were considered to further analysis. A 100-fold dilution of the PCR product was subsequently used as template for the second PCR reaction using the primers described in the section: analysis of mRNA expression by B and plasma cells. Amplification of the respective transcript was verified on an agarose gel.

Histology. For immunostaining, 1- to 2-μm sections of formalin-fixed, paraffin-embedded tissue were cut, deparaffinized and subjected to a heat-induced epitope retrieval step. Slides were rinsed in cool running water and washed in Tris-buffered saline (pH 7.4) before incubation with primary antibodies against CD3 (cat number N1580, Dako, Glostrup, Denmark, dilution 1:10), and F4/80 (clone BM8, eBioscience, dilution 1:50) for 30 min, followed by biotinylated donkey anti-rat or donkey anti-rabbit (cat. numbers 712-065-153 and 711-065-152, Dianova, Hamburg, Germany) secondary antibodies. The streptavidin-AP kit (cat. number K5005, Dako) was used for detection. As negative control, primary antibody was omitted.

Detection of serum antibodies by ELISA. To quantify Salmonella-specific or NP-OVA-specific antibodies, diluted sera were incubated on 96-well plates coated with 5×10^6 heat-killed *S. typhimurium* per well or 50 μg ml^{-1} NP(15)-BSA (Biosearch Technologies), respectively. Detection was done with alkaline phosphatase-conjugated anti-IgM (cat number 1020-04), anti-IgG (cat number 1030-04), anti-IgG1 (cat number 1070-04), anti-IgG2b (cat number 1090-04), anti-IgG2c (cat number 1079-04), and anti-IgG3 (cat number 1100-04) antibodies (all from Southern Biotechnology Associates).

Detection of mouse IL-27 p28 subunit by ELISA. The concentration of mouse IL-27 p28 subunit was quantified using the mouse IL-27 p28 Quantikine ELISA Kit (cat number M2728, R&D Systems), according to the manufacturer's instructions.

Isolation of CNS-infiltrating cells. CNS single-cell suspension was obtained by collagenase digestion of brain and spinal cord. Infiltrating leukocytes were separated from debris and tissue cells using Ficoll centrifugation. Cell numbers were determined by FACS. Cells were characterized by flow cytometry after staining for CD4 (clone RM4-5), CD11b (clone M1/70), Ly6G (clone 1A8) and Foxp3 (clone FJK16 s).

Treg suppression assay. CD4$^+$CD25$^+$ T cells (Treg) were isolated from B$^{p35^{-/-}}$ and B^{WT} mice on day 10 post-EAE induction, and compared for their capacity to suppress the proliferation of CD4$^+$CD25$^-$ T cells (Teff) isolated from naive C57BL/6 mice *in vitro*, as previously described[31].

ELISPOT Assay. Sorted B cells (CD19$^+$CD138$^-$), and plasma cell subsets (CD138^{int}CD22$^+$, CD138^{hi}CD22$^+$, and CD138^{hi}CD22$^-$ cells) or total plasma cells (CD138$^+$) were seeded at a starting number of 10^4 cells per well, with seven successive threefold serial dilutions, in 96-well flat-bottom EIA/RIA high-binding plate (Millipore) pre-coated with anti-mouse Ig(H+L) chain (5 μg ml^{-1}; Southern Biotechnology Associates, cat number 1010-01). After 3 h incubation, plates were washed, and incubated with alkaline phosphatase-conjugated anti-IgM or anti-IgG antibodies overnight at 4 °C (Southern Biotechnology Associates, cat numbers 1020-04 and 1030-04). ELISPOT were then developed using BCIP/NBT substrate (Gene Tex Inc.).

Stimulation and characterization of plasma cells and B cells. Purified plasma cells and B cells were seeded at 5×10^5 cells per well on 96-well flat-bottom plates and stimulated with PMA plus ionomycin, LPS (1 μg ml^{-1}; *Escherichia coli* serotype 055:B5; Sigma-Aldrich), agonistic anti-CD40 antibody (10 μg ml^{-1}; clone FGK-45, produced in house), anti-IgM (5 μg ml^{-1}, cat number 115-006-075, Jackson ImmunoResearch Laboratories, USA), IL-4 (20 ng ml^{-1}; R & D Systems GmbH), IL-5 (20 ng ml^{-1}; eBioscience), IL-6 (20 ng ml^{-1}; R & D Systems GmbH), IL-21 (20 ng ml^{-1}; R & D Systems GmbH), and indicated combinations. After 24 h, supernatants were harvested for the detection of IL-10 and IL-6 concentration by Bio-Plex (Bio-Rad, USA); cells were subjected to flow cytometry for the quantification of GFP-positive cells. Characterizations were done by flow cytometry after staining for CD19 (clone 1D3, BD Pharmingen), CD138 (clone 281-2, BD Pharmingen), IgM (cat number 1020-02, SouthernBiotech), IgD (clone 217-170, BD Pharmingen), CD80 (clone 16-10A1, BD Pharmingen), CD86 (clone GL1, BD Pharmingen), MHCII (clone M5/114, in house), CD40 (clone 3/23, BD Pharmingen), CD69 (clone H1.2F3, eBioscience), CD44 (clone 1M7, in house), CD43 (clone S7, BD Pharmingen), CD28 (clone E18, Biolegend), TACI (clone 8F10, BD Pharmingen), CXCR4 (clone 2B11, BD Pharmingen), CD1d (clone 1.B1, in house) and Tim1 (clone RMT1-4, Biolegend).

Validation of chimaeras. B$^{Ebi3^{-/-}}$ and corresponding B^{WT} chimaeras were used as an example to demonstrate the validity of the chimaera system, that is, that the deficiency in the gene of interest is restricted to B cells, and complete in that compartment in B$^{X^{-/-}}$ mice. To this end, B cells, CD11b$^+$ cells and CD4$^+$ T cells were purified from B$^{Ebi3^{-/-}}$ and corresponding B^{WT} chimaeras. Briefly, splenocytes from B$^{Ebi3^{-/-}}$ and B^{WT} mice were subjected to CD19 positive selection using magnetic cell sorting. The CD19$^+$ fraction was subsequently stained for B220 (clone RA3-6B2), CD11b (clone M1/70), CD11c (clone N418), CD4 (clone GK1.5), and CD8 (clone 53.6.72), and FACS-sorted for B220$^+$CD11b$^-$CD11c$^-$CD4$^-$CD8$^-$ cells, yielding >99% pure B cells. The CD19$^-$ fraction obtained from the magnetic sort was stained, and used to FACS-sort CD4$^+$B220$^-$CD11b$^-$ cells, and CD11b$^+$B220$^-$CD4$^-$ cells, resulting in >97–98% pure CD4$^+$ T cells and CD11b$^+$ cells, respectively. All sorted populations as well as the remaining non-T/B/CD11b$^+$ cells (denoted as non-T, B, M cells) were lysed and genomic DNA was extracted using the DNeasy Blood & Tissue Kit (Qiagen), according to the manufacturer's instructions. The amounts of genomic DNA present in these samples were equilibrated by real time PCR using the *Mog* gene as standard with the primer pair: forward 5′-AGGAAGGGACATGCAGCCGGA-3′; reverse 5′-CTGC ATAGCTGCATGACAACTG-3′. Wild-type *Ebi3* gene was then amplified by conventional PCR with the following primers: forward 5′-AACCTCAGGCCA GGCAGT-3′; reverse 5′-TTCCGTAGGCCATGTAGGAC-3′, in order to test for the presence of the wild-type *Ebi3* allele in the different cell fractions.

Additional reagents. Antibodies used in this study also included anti-Ly6C (clone AL21, cat number 557359, BD Pharmingen), anti-IFN-γ (clone XMG1.2, BD Pharmingen), anti-CD154 (cat number 130-092-105, Miltenyi Biotech), anti-CD62L (MEL14, in house).

Statistics. Statistical analysis was performed using GraphPad Prism (version 5.02 for Windows, GraphPad Software, USA). EAE data distribution did not differ from normal distribution, as evaluated using Kolmogorov–Smirnov test. Equality of variances between groups was assessed before analyses by ANOVA or *t*-test. Groups were compared using ANOVA, two-tailed *t*-test, or Wilcoxon test, as indicated in figure legends. The *t*-tests were modified using Welch's correction in case of unequal variance. One-way and two-way ANOVA were followed by Bonferroni post-test. No samples were excluded from analysis. Statistical analysis of the gene array data are described in the section gene array hybridization and data analysis.

29. Biesen, R. *et al.* Sialic acid-binding Ig-like lectin 1 expression in inflammatory and resident monocytes is a potential biomarker for monitoring disease activity and success of therapy in systemic lupus erythematosus. *Arthritis Rheum.* **58,** 1136–1145 (2008).
30. Saeed, A. I. *et al.* TM4: a free, open-source system for microarray data management and analysis. *Biotechniques* **34,** 374–378 (2003).
31. Hoehlig, K. *et al.* Activation of CD4$^+$ Foxp3$^+$ regulatory T cells proceeds normally in the absence of B cells during EAE. *Eur. J. Immunol.* **42,** 1164–1173 (2012).

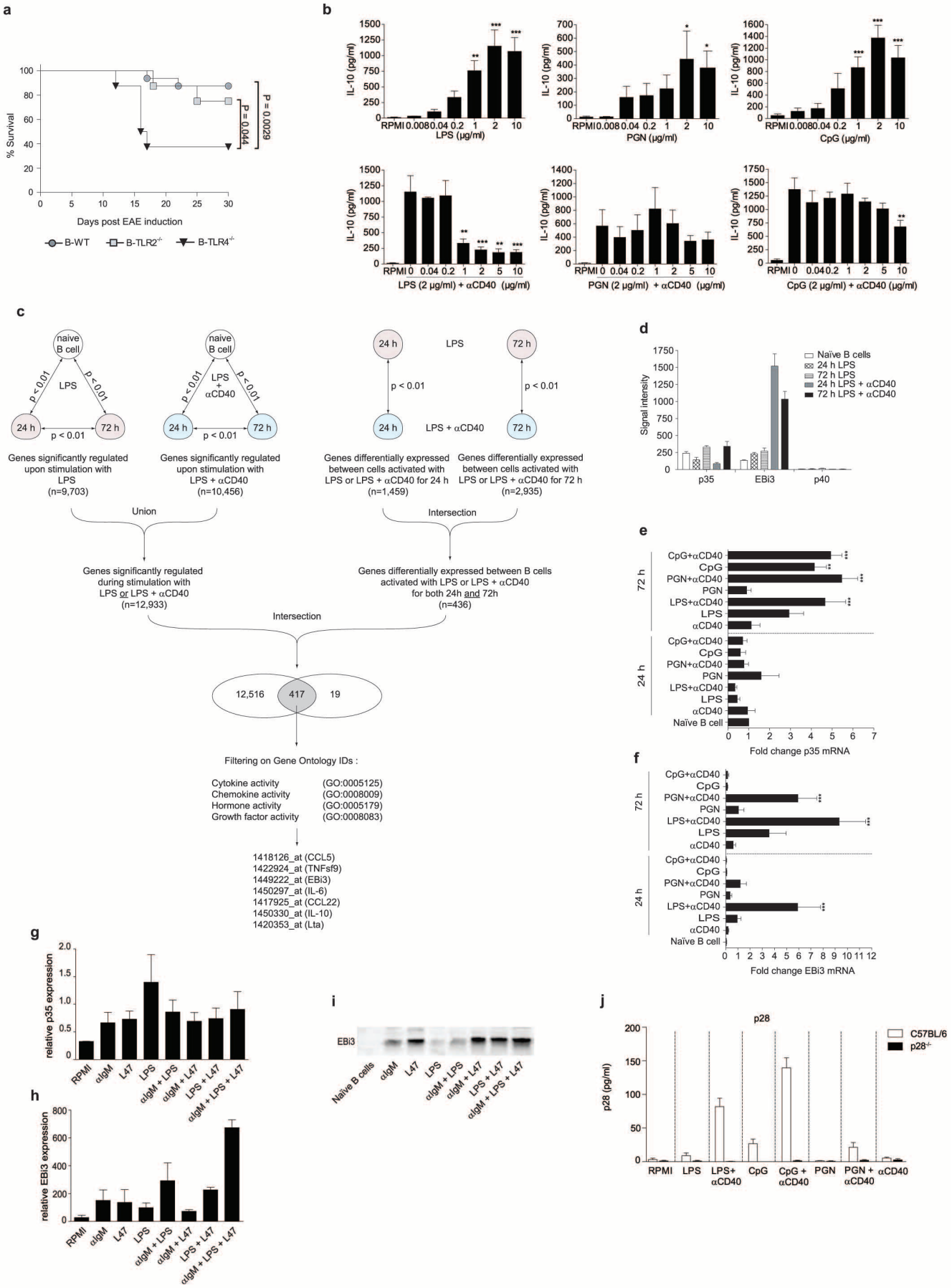

Extended Data Figure 1 | Gene array analysis and IL-35 secretion by B cells activated *in vitro*. **a**, EAE was induced in $B^{Tlr2^{-/-}}$ (squares), $B^{Tlr4^{-/-}}$ (triangles) and B^{WT} (circles) mice (see Fig. 1). Animals showing a body weight loss >20% and/or sustained front leg impairment were killed in accordance with ethical regulations. Survival curves were compared using Wilcoxon test. **b**, In the top panels, splenic B cells from C57BL/6 mice were stimulated with lipopolysaccharides (LPS), peptidoglycan (PGN) or CpG DNA oligonucleotides for 72 h, as indicated, and IL-10 concentrations in supernatants were determined by Bio-Plex. Results from stimulated cells were compared to unstimulated B cells (RPMI) using one-way ANOVA followed by Bonferroni post-test (***$P < 0.001$; **$P < 0.01$; *$P < 0.05$; mean ± s.e.m.); in the bottom panels, splenic B cells were simultaneously activated with anti-CD40 (clone FGK-45; in indicated amounts) and LPS (2 μg ml^{-1}), PGN (2 μg ml^{-1}) or CpG (2 μg ml^{-1}). Supernatants were collected after 72 h and analysed for IL-10 content by Bio-Plex. Data shown are pooled from three independent experiments (mean ± s.e.m.). Results from B cells stimulated with LPS, CpG or PGN alone were compared to B cells co-stimulated with anti-CD40 using one-way ANOVA followed by Bonferroni post-test (***$P < 0.001$; **$P < 0.01$; *$P < 0.05$). **c**, Affymetrix MG 430 2.0 whole genome arrays were performed in quadruplicates for naive B cells, B cells activated by TLR4 for 24 h and 72 h, and B cells activated by TLR4 plus CD40 for 24 h and 72 h (20 arrays in total). To obtain genes significantly regulated upon stimulation with LPS, the expression profiles of naive B cells, B cells activated with LPS for 24 h, and B cells activated with LPS for 72 h were compared to each other, generating three lists of differentially expressed Affymetrix IDs (referred to as genes in this figure), whose union provided a set of $n = 9{,}703$ Affymetrix IDs differentially expressed during LPS activation. A similar analysis yielded a set of $n = 10{,}456$ Affymetrix IDs differentially expressed during LPS plus anti-CD40 activation. The union of these two sets was computed to obtain the list of Affymetrix IDs modulated during B-cell stimulation with LPS or LPS plus anti-CD40 ($n = 12{,}933$). To focus on genes differentially expressed between B cells activated with LPS or LPS plus anti-CD40, the expression profiles of B cells activated with LPS or LPS plus anti-CD40 for 24 h were compared to each other. A similar analysis was done for B cells activated for 72 h. The intersection of these two sets provided the list of Affymetrix IDs differentially expressed between LPS-activated and LPS-activated plus anti-CD40-activated B cells at both 24 h and 72 h (this was done to identify the Affymetrix IDs with long-term differential expression) ($n = 436$). The intersection of the set $n = 12{,}933$ with the set $n = 436$ gave a list of 417 Affymetrix IDs, which was further filtered on Gene Ontology to extract the Affymetrix IDs corresponding to secreted factors, yielding a final list of 7 genes. **d**, Signal intensities of *p35*, *Ebi3* and *p40* mRNA expression were calculated using the values of the Affymetrix arrays. Data show mean ± s.e.m. **e**, **f**, Splenic murine B cells were stimulated with LPS (1 μg ml^{-1}), PGN (10 μg ml^{-1}), CpG ODN 1826 (1 μg ml^{-1}), and anti-CD40 (clone FGK-45; 10 μg ml^{-1}), alone or in combination, as indicated, for 24 h or 72 h. *p35* (**e**) and *Ebi3* (**f**) mRNA expression was then quantified by real-time PCR. Data compile three independent experiments (mean ± s.e.m.). For statistical analysis, one-way ANOVA test followed by Bonferroni post-test was performed comparing each activated B-cell sample to naive B cells (***$P < 0.001$; **$P < 0.01$; mean ± s.e.m.). **g**–**i**, Splenic murine B cells were stimulated for 72 h with anti-IgM (F(ab′)2 goat anti-mouse IgM; Jackson ImmunoResearch; 5 μg ml^{-1}), LPS (1 μg ml^{-1}) and L47 cells (5×10^4 cells, irradiated), alone or in combinations, as indicated. **g**, **h**, Levels of *p35* and *Ebi3* mRNA expression were quantified by real-time PCR. Data show compilation of three independent experiments (mean ± s.e.m.). **i**, Splenic murine B cells were activated as indicated for 72 h, and treated with GolgiStop for the last 4 h of culture. B-cell lysates were separated on SDS–PAGE gel and blotted with anti-EBI3 antibody. Data show representative results from three independent experiments. **j**, Splenic B cell from C57BL/6 and *p28* mice were stimulated with LPS (1 μg ml^{-1}), CpG (1 μg ml^{-1}), PGN (10 μg ml^{-1}), anti-CD40 (10 μg ml^{-1}), alone or in combination, as indicated, for 72 h. p28 concentrations in culture supernatants were determined by ELISA. Data shown (mean ± s.em) are pooled from four independent experiments.

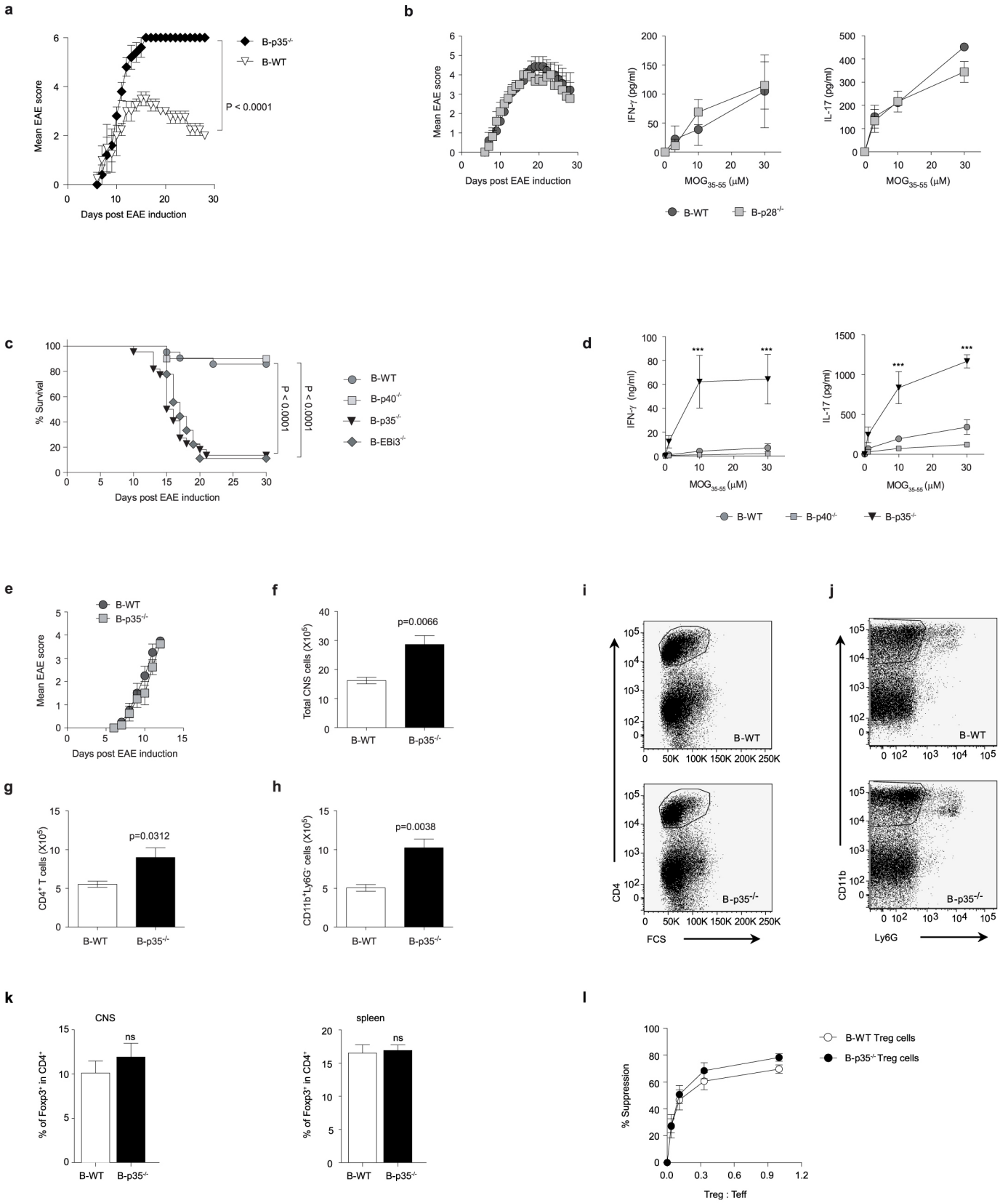

Extended Data Figure 2 | Characterization of immune reponses during EAE in mice lacking IL-35 expression in B cells. **a**, EAE was induced in $B^{p35^{-/-}}$ (black diamonds, $n = 5$) and corresponding B^{WT} mice (white triangles, $n = 4$). Data show clinical EAE scores (mean ± s.e.m.) from two independent experiments. Cumulative disease scores were compared using two-tailed unpaired *t*-test. **b**, EAE was induced in $B^{p28^{-/-}}$ (grey squares; $n = 10$) and corresponding B^{WT} mice (dark grey circles, $n = 10$). Splenocytes were collected from mice on day 28 after EAE induction, and re-stimulated individually for 48 h with $MOG_{35–55}$. Supernatants were analysed by ELISA to determine concentrations of IFN-γ (middle) and IL-17 (right). Data (mean ± s.e.m.) are pooled from two independent experiments. **c**, EAE was induced in $B^{p35^{-/-}}$ (triangles), $B^{Ebi3^{-/-}}$ (diamonds), $B^{p40^{-/-}}$ (squares), and B^{WT} (circles) mice (see Fig. 2). Animals showing a body weight loss > 20% and/or sustained front leg impairment were killed in accordance with ethical regulations. Survival curves were compared using Wilcoxon test. **d**, Splenocytes were collected from $B^{p35^{-/-}}$, $B^{p40^{-/-}}$, and B^{WT} mice on day 28 after EAE induction (see Fig. 2a), and pooled before re-stimulation for 48 h with $MOG_{35–55}$. Culture supernatants were analysed by ELISA to determine concentrations of IFN-γ (left) and IL-17 (right). Data show representative results from two independent experiments. Statistical analysis was performed using the two-way-ANOVA test followed by a Bonferroni post-test (*$P < 0.05$, **$P < 0.01$; ***$P < 0.001$; mean ± s.e.m.). Results of analysis are shown for B^{WT} versus $B^{p35^{-/-}}$ comparison. **e–j**, EAE was induced in $B^{p35^{-/-}}$ (grey squares; $n = 8$) and corresponding B^{WT} mice (dark grey circles; $n = 8$) and mice were killed at day 12 post-EAE induction to analyse accumulation of immune cells in CNS. Data show clinical EAE scores (mean ± s.e.m.) (**e**). **f–h**, Mononuclear cells were isolated from CNS (brain plus spinal cord) of individual mice shown in (**e**), and numbers of total cells (**f**), $CD4^+$ T cells (**g**) and $CD11b^+Ly6G^-$ macrophages (**h**) were quantified by flow cytometry. Data shown (mean ± s.e.m.) are pooled from two independent experiments. Results were compared using two-tailed unpaired *t*-test with Welch's correction in case of inequal variances. **i**, **j**, Representative FACS plots of $CD4^+$ T cells and $CD11b^+Ly6G^-$ macrophages, respectively. **k**, Frequencies of $Foxp3^+$ Treg cells among $CD4^+CD8^-$ T cells in CNS at day 12 post-EAE induction (left panel), and in spleen at day 10 post-EAE induction (right panel) as determined by flow cytometry. Data shown in the left panel (mean ± s.e.m.) are pooled from two independent experiments with 10 mice per group in total. Data shown in the right panel (mean ± s.e.m.) are representative of three independent experiments with 9 mice per group in total. Results were compared using two-tailed unpaired *t*-test. *P* values >0.05 are indicated by ns. **l**, Treg suppression assay. $CD4^+CD25^+$ T cells (Treg) were FACS-sorted from pooled spleen and lymph nodes of $B^{p35^{-/-}}$ and corresponding B^{WT} mice on day 10 post-EAE induction, and then co-cultured at the indicated ratios with 2×10^4 $CD4^+CD25^-$ T cells (Teff) isolated from naive C57BL/6 mice in presence of 1×10^5 irradiated splenocytes and 0.1 μg ml^{-1} anti-CD3 (clone 145-2C11). Proliferation was measured after 64 h of culture by incorporation of $[^3H]$thymidine, and plotted as suppression percentage defining as 100% the proliferation values obtained for control cultures without Treg cells. Data (mean ± s.e.m.) are pooled from two independent experiments.

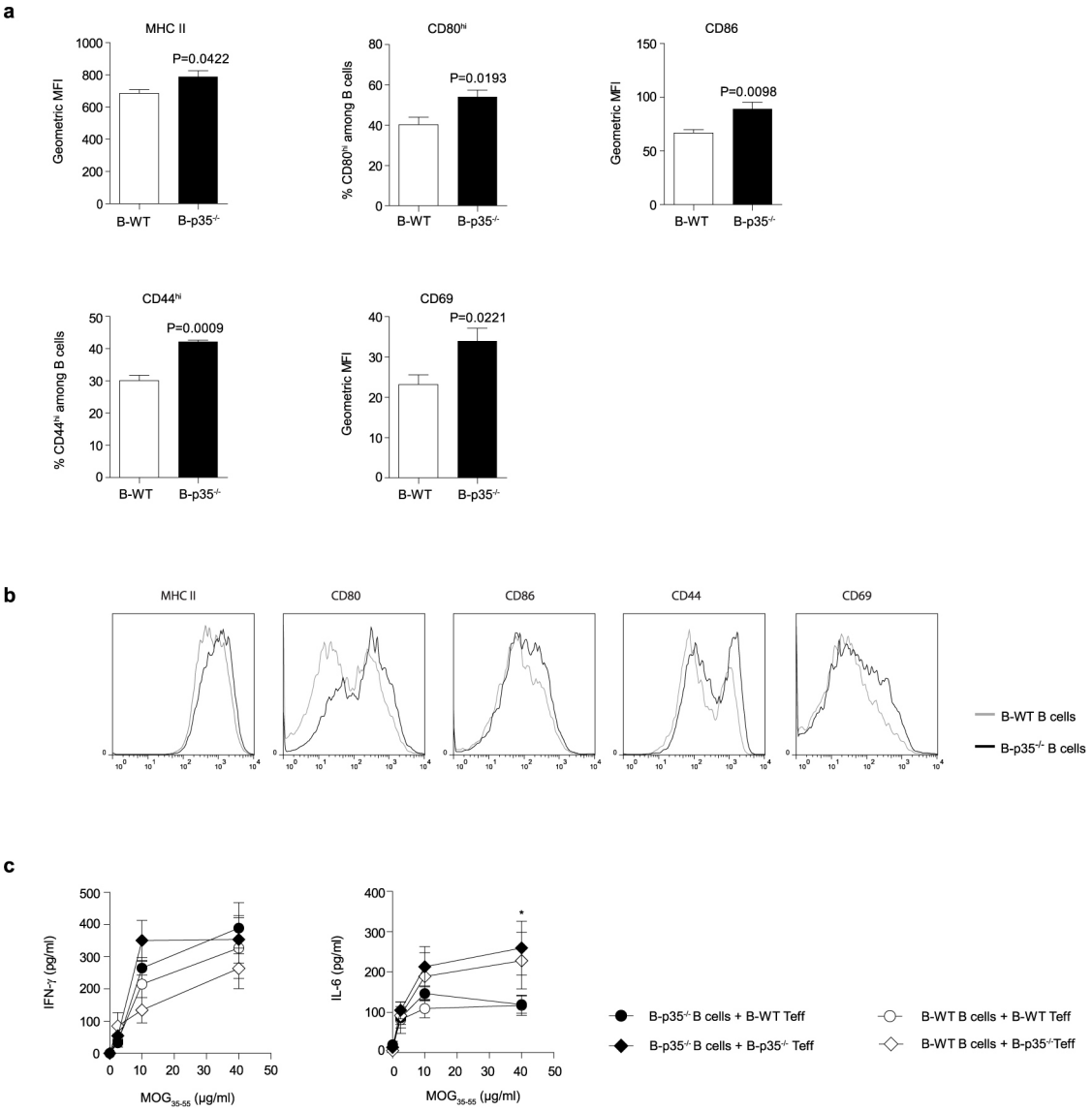

Extended Data Figure 3 | Lack of IL-35 production by B cells results in increased activation of B cells during EAE. **a**, EAE was induced in $B^{p35^{-/-}}$ ($n = 6$) and corresponding B^{WT} mice ($n = 6$). Mice were killed on day 10 after immunization and splenic B cells were analysed by flow cytometry for surface expression of antigen-presenting molecules (MHC II), co-stimulatory molecules (CD80, CD86), and activation markers (CD44, CD69). MFI, mean fluorescence intensity. Data (mean ± s.e.m.) are pooled from two independent experiments. Results were compared using two-tailed unpaired *t*-test with Welch's correction in case of inequal variances. **b**, Representative histogram plots showing expression of these molecules on wild-type and p35-deficient B cells. Dead cells were excluded using propidium iodide. **c**, EAE was induced in $B^{p35^{-/-}}$ and corresponding B^{WT} mice. B cells and $CD4^{+}CD25^{-}$ T cells (Teff) were isolated from pooled lymph nodes and spleens on day 10 after immunization. To test the APC function of B cells (see Fig. 2), 5×10^5 B cells from $B^{p35^{-/-}}$ or B^{WT} mice were then cultured with 1×10^4 Teff cells from $B^{p35^{-/-}}$ or B^{WT} mice in presence of MOG_{35-55}, as indicated. Culture supernatants were collected after 48 h, and analysed by Bio-Plex to determine concentrations of IFN-γ (left) and IL-6 (right). Data (mean ± s.e.m.) are pooled from two independent experiments. Results were compared using two-way ANOVA followed by Bonferroni post-test (*$P < 0.05$). Results of analysis are shown for comparison, B^{WT} B cells plus B^{WT} T cells versus $B^{p35^{-/-}}$ B cells plus $B^{p35^{-/-}}$ T cells for IL-6.

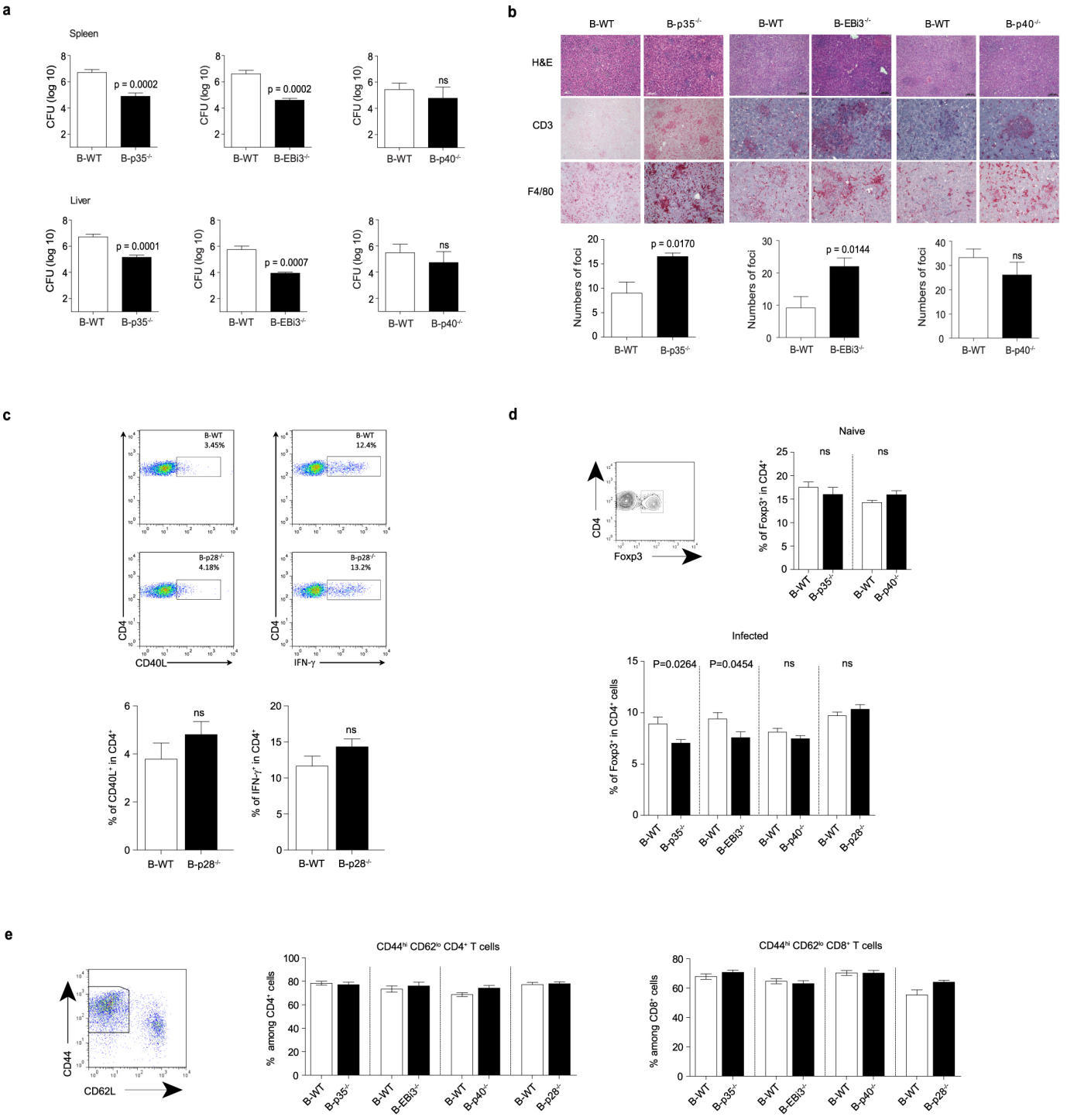

Extended Data Figure 4 | Bacterial burden and T-cell activation in mice lacking IL-35 production by B cells during *Salmonella* infection. **a**, $B^{p35^{-/-}}$, $B^{Ebi3^{-/-}}$, $B^{p40^{-/-}}$ and corresponding B^{WT} mice were infected intravenously with virulent *Salmonella* strain SL1344 (100 c.f.u.). Bacterial loads in spleens (top) and livers (bottom) were determined on day 6 post-infection (p.i). Data (mean ± s.e.m.) are pooled from two independent experiments. Numbers of mice analysed: $B^{p35^{-/-}}$ ($n = 6$) and corresponding B^{WT} mice ($n = 8$), $B^{Ebi3^{-/-}}$ ($n = 5$) and corresponding B^{WT} mice ($n = 5$), $B^{p40^{-/-}}$ ($n = 6$) and corresponding control B^{WT} mice ($n = 5$). Data were analysed with two-tailed unpaired *t*-test. *P* values > 0.05 are indicated by ns. **b**, Top shows liver histochemistry of total infiltrating cells (haematoxylin and eosin; H&E), T cells (CD3), and macrophages (F4/80) at day 6 p.i.; bottom, numbers of inflammatory foci per liver section on day 6 p.i. Data (mean ± s.e.m.) are pooled from two independent experiments. Numbers of mice analysed: $B^{p35^{-/-}}$ ($n = 6$) and corresponding B^{WT} mice ($n = 8$), $B^{Ebi3^{-/-}}$ ($n = 7$) and corresponding B^{WT} mice ($n = 5$), $B^{p40^{-/-}}$ ($n = 7$) and corresponding B^{WT} mice ($n = 8$). Data were compared using two-tailed unpaired *t*-test with Welch's correction in case of inequal variances. *P* values > 0.05 are indicated by ns. **c**, $B^{p28^{-/-}}$ ($n = 6$) and corresponding B^{WT} ($n = 6$) mice were infected intravenously with attenuated *Salmonella* (strain SL7207). On day 21 p.i. bone marrow (BM) cells were isolated from individual mice, and re-stimulated for 6 h with heat-killed *Salmonella* before staining for surface CD4, and intracellular CD40L or IFN-γ. (top). Representative FACS plots showing CD40L and IFN-γ expression by $CD4^+$ T cells, after gating on $CD4^+$ cells. Bottom, frequencies of $CD40L^+$ (left) and IFN-γ^+ (right) cells among $CD4^+$ T cells in BM (mean ± s.e.m.). Data are pooled from two independent experiments. Data were compared using two-tailed unpaired *t*-test. *P* values > 0.05 are indicated by ns. **d**, Representative FACS plot shows Foxp3 expression by splenic $CD4^+$ T cells from a B^{WT} mouse on day 21 p.i. with attenuated *Salmonella* (strain SL7207); (top right) frequency of $Foxp3^+$ Treg cells among $CD4^+$ T cells in spleens of naive $B^{p35^{-/-}}$ ($n = 5$) and corresponding B^{WT} mice ($n = 5$), $B^{p40^{-/-}}$ ($n = 7$) and corresponding B^{WT} mice ($n = 7$); (bottom) frequency of $Foxp3^+$ Treg cells among $CD4^+$ T cells on day 21 p.i. with attenuated *Salmonella* (strain SL7207) in spleens of $B^{p35^{-/-}}$ ($n = 8$) and corresponding B^{WT} mice ($n = 8$), $B^{Ebi3^{-/-}}$ ($n = 10$) and corresponding B^{WT} mice ($n = 10$), $B^{p40^{-/-}}$ ($n = 15$) and corresponding B^{WT} mice ($n = 9$), $B^{p28^{-/-}}$ ($n = 6$) and corresponding B^{WT} mice ($n = 6$). Data (mean ± s.e.m.) are pooled from two independent experiments. Data were analysed with two-tailed unpaired *t*-test. *P* values >0.05 are indicated by ns. **e**, Mice were infected as in (**d**) and frequency of activated $CD44^{hi}CD62L^{lo}$ $CD4^+$ and $CD8^+$ T cells were determined by flow cytometry. Representative FACS plot shows expression of CD44 and CD62L by live (PI negative) $CD4^+$ T cells. Graphs show frequencies of $CD44^{hi}CD62L^{lo}$ cells among $CD4^+$ T cells (left) and $CD8^+$ T cells (right). Data (mean ± s.e.m.) are pooled from two independent experiments. Numbers of mice analysed: $B^{p35^{-/-}}$ ($n = 14$) and corresponding B^{WT} mice ($n = 12$), $B^{Ebi3^{-/-}}$ ($n = 10$) and corresponding B^{WT} mice ($n = 10$), $B^{p40^{-/-}}$ ($n = 15$) and corresponding B^{WT} mice ($n = 9$), $B^{p28^{-/-}}$ ($n = 6$) and corresponding B^{WT} mice ($n = 6$).

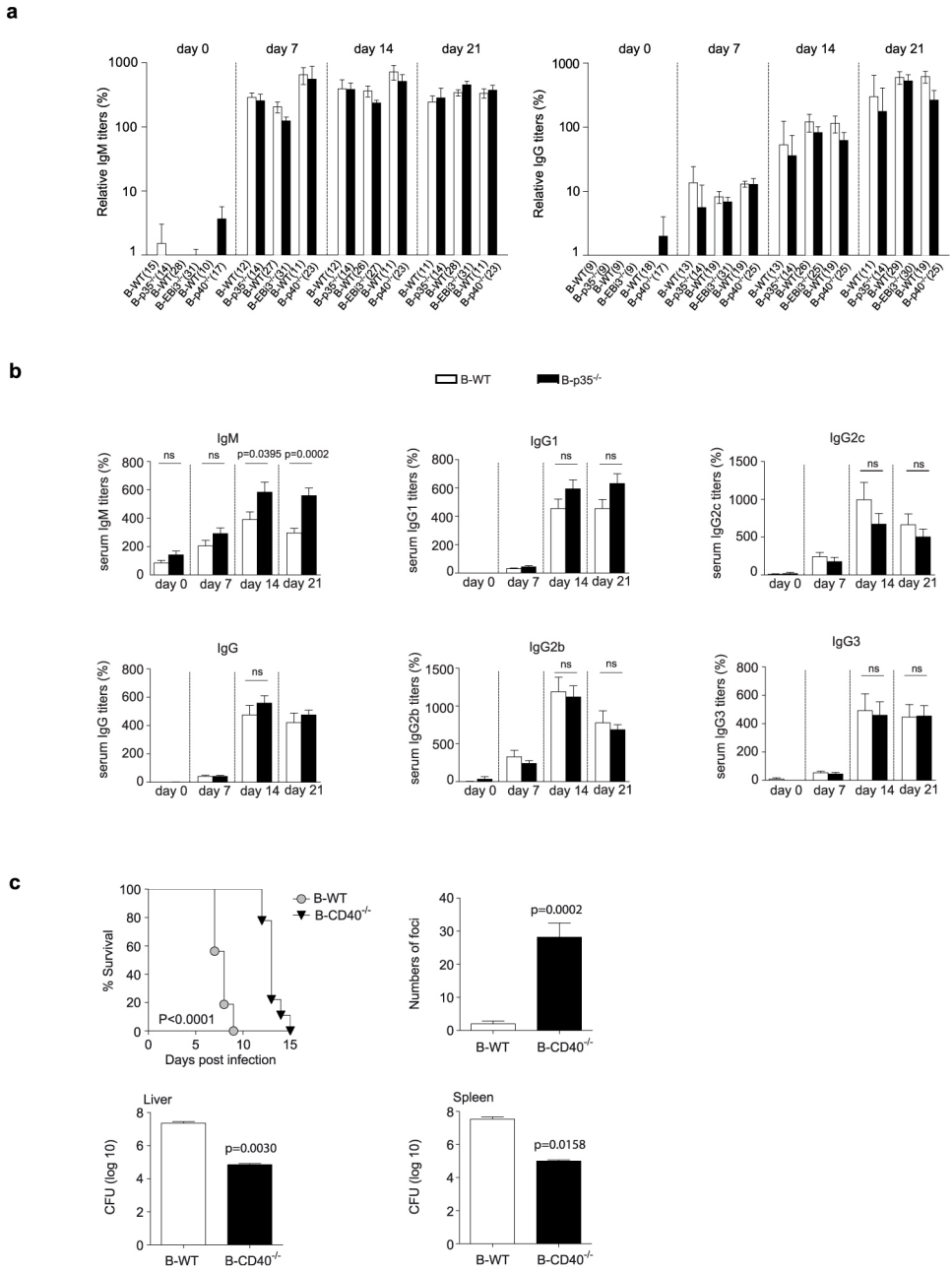

Extended Data Figure 5 | Role of IL-35 and CD40 expression by B cells during *Salmonella* infection. **a**, $B^{p35^{-/-}}$, $B^{Ebi3^{-/-}}$, $B^{p40^{-/-}}$ and their corresponding B^{WT} mice were infected with attenuated *Salmonella* (strain SL7207). Relative titres of *Salmonella*-reactive IgM and IgG in serum were determined by ELISA. Data (mean ± s.e.m.) are pooled from three independent experiments. Numbers in brackets indicate the numbers of mice analysed for each measurement. **b**, $B^{p35^{-/-}}$ ($n = 17$) and corresponding B^{WT} mice ($n = 16$) were immunized with 200 μg NP-OVA in alum intraperitoneally. Relative titres of NP(15)-BSA-reactive antibodies in serum were determined by ELISA. Data (mean ± s.e.m.) are pooled from three independent experiments. Results were compared using two-tailed unpaired *t*-test. *P* values >0.05 are indicated by ns. **c**, Mice were infected with 100 c.f.u. of virulent *Salmonella*. Upper left shows survival curves of $B^{Cd40^{-/-}}$ ($n = 9$) and corresponding B^{WT} mice ($n = 16$). Data are pooled from two independent experiments. Survival curves were compared using Wilcoxon test. Upper right, numbers of inflammatory foci per liver section were determined on day 5 p.i. Lower panel, bacterial loads in liver (left) and spleen (right) were determined on day 5 p.i. Data (mean ± s.e.m.) are pooled from two independent experiments. Numbers of mice analysed: $B^{Cd40^{-/-}}$ ($n = 12$), and corresponding B^{WT} mice ($n = 13$). Results were analysed using two-tailed unpaired *t*-test with Welch's correction.

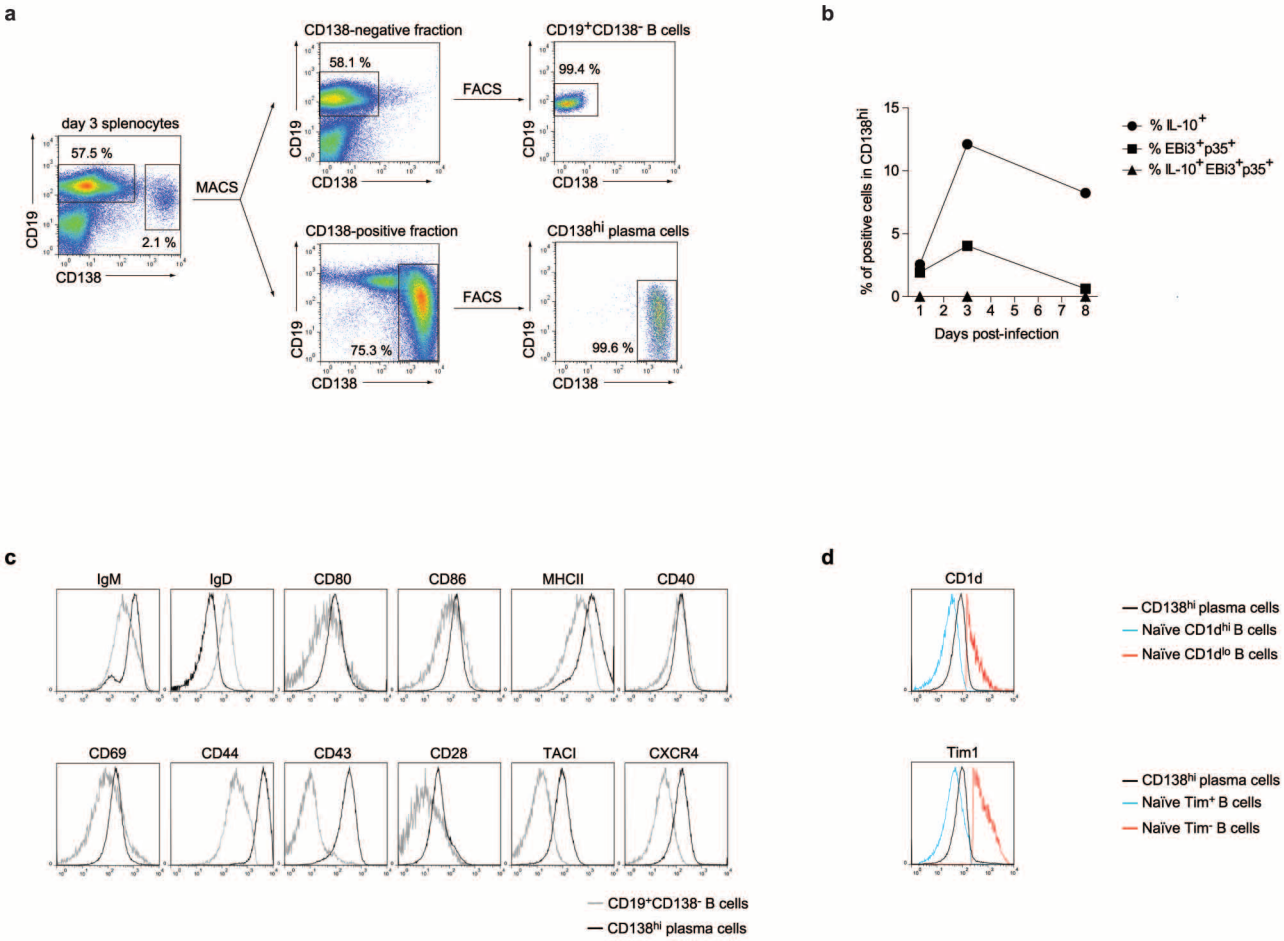

Extended Data Figure 6 | Characterization of IL-10- and IL-35-expressing plasma cells during *Salmonella* infection. **a**, **b**, C57BL/6 mice were infected intravenously with attenuated *Salmonella* (strain SL7207; 10^7 c.f.u.). On indicated days p.i., $CD138^{hi}$ plasma cells and $CD19^+CD138^-$ B cells were isolated from spleen through magnetic and FACS procedures. **a**, Strategy for isolation of $CD138^{hi}$ plasma cells and $CD19^+CD138^-$ B cells: splenocytes were stained with anti-CD138-PE followed by labelling with magnetic anti-PE microbeads, and magnetic separation on autoMACS (Miltenyi Biotech). The obtained CD138-positive and CD138-negative fractions were stained for CD19, CD138 and CD11b/CD11c/TCR-β/DAPI. $CD138^{hi}CD11b^-CD11c^-TCR\text{-}\beta^-DAPI^-$ and $CD19^+CD138^-CD11b^-CD11c^-TCR\text{-}\beta^-DAPI^-$ cells were then isolated from CD138-positive and CD138-negative fraction, respectively, by FACS, as bulk or single cells. Numbers in FACS plots indicate the percentages of $CD19^+CD138^-$ B cells and $CD138^{hi}$ plasma cells in total splenocytes on day 3 after challenge (left plots), after magnetic isolation (middle plots), and after FACS isolation (right plots). **b**, Single $CD138^{hi}$ cells were isolated on indicated days, and analysed by single cell-PCR using a mix of primers for β-actin, *Il10*, *p35* and *Ebi3*. Only cells giving a positive signal for β-actin were included in the calculations shown. Data show frequencies of $CD138^{hi}$ cells that gave a positive signal for *Il10*, both *p35* and *Ebi3*, or *Il10* and *p35* and *Ebi3*. Numbers of cells tested: day 1 (181 cells; 86% positive for β-actin), day 3 (156 cells; 79% positive for β-actin) and day 8 (163 cells; 97% positive for β-actin). Cells were obtained from two independent experiments. **c**, **d**, $CD138^{hi}$ plasma cells and $CD19^+CD138^-$ B cells were enriched by magnetic isolation (as described in **a**) from spleen of C57BL/6 mice on day 3 after infection with attenuated *Salmonella* (SL7207; 10^7 c.f.u.). **c**, Data show expression levels of selected surface receptors on live ($DAPI^-$) $CD138^{hi}$ plasma cells and $CD19^+CD138^-$ B cells. Cells were gated as in **a** (middle panels), and analysed by flow cytometry. **d**, Levels of CD1d and Tim-1 expressed by $CD138^{hi}$ cells were compared to those found respectively on $CD1d^{hi}$ and $CD1d^{lo}$ B cells, and on $Tim1^+$ and $Tim1^-$ B cells from spleen of naive C57BL/6 mice. Data show representative results from 2–5 independent experiments.

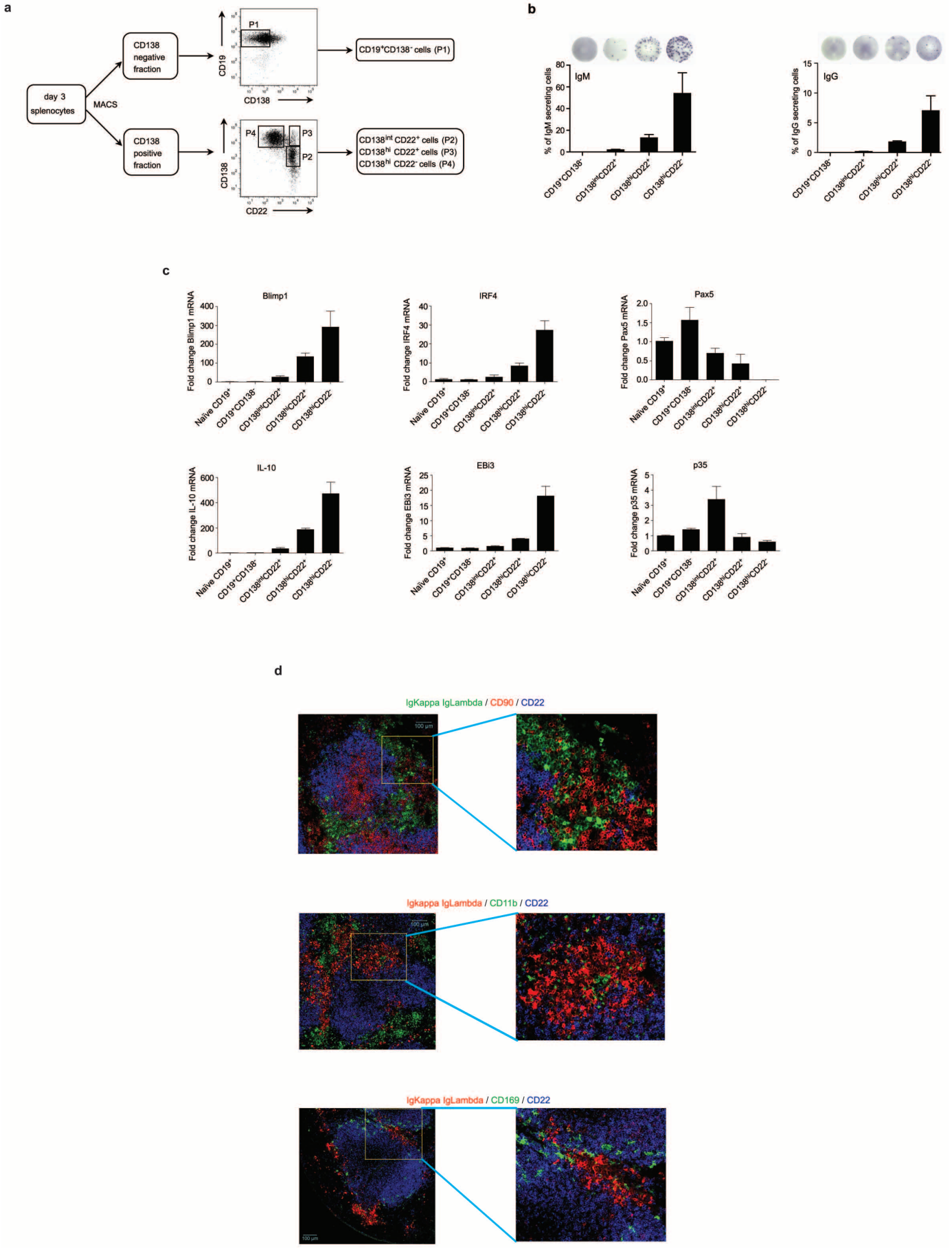

Extended Data Figure 7 | Characterization of plasma cells during *Salmonella* infection. **a**, $CD138^{hi}$ plasma cells and $CD19^{+}CD138^{-}$ B cells were magnetically enriched from spleens of C57BL/6 mice on day 3 after infection with attenuated *Salmonella* (SL7207; 10^7 c.f.u.). $CD19^{+}CD138^{-}$ B cells (P1) were then isolated from the CD138-negative fraction by FACS. $CD138^{int}CD22^{+}$ (P2), $CD138^{hi}CD22^{+}$ (P3), and $CD138^{hi}CD22^{-}$ (P4) were isolated from the CD138-positive fraction by FACS. **b**, Frequencies of IgM- and IgG-secreting cells among B cells ($CD19^{+}CD138^{-}$) and each of these plasma cell subsets ($CD138^{int}CD22^{+}$, $CD138^{hi}CD22^{+}$, $CD138^{hi}CD22^{-}$) were determined by ELISPOT assay. A compilation of two independent experiments is shown (mean ± s.e.m.). **c**, *Blimp1*, *Irf4*, *Pax5*, *Il10*, *Ebi3* and *p35* mRNA expression was quantified by real-time PCR in these populations. Naive splenic B cells (naive $CD19^{+}$) were isolated from unchallenged C57BL/6 mice by magnetic selection. Data show the compilation of three independent experiments (mean ± s.e.m.). **d**, Plasma cells accumulate in splenic red pulp aggregates adjacent to white pulp areas on day 3 after *Salmonella* infection. C57BL/6 mice were infected intravenously with attenuated *Salmonella* (SL7207; 10^7 c.f.u.), and spleens were harvested 3 days later. Spleen sections (7 μm) were stained with: top panels: anti-Ig-κ (clone 187.1; green), anti-Igλ (clone SL136; green), anti-CD90 (clone T24; red) and anti-CD22 (clone OX-97; blue); middle panels: anti-Ig-κ (clone 187.1; red), anti-Igλ (clone SL136; red), anti-CD11b (clone M1/70; green), and anti-CD22 (clone OX-97; blue); bottom panels: anti-Ig-κ (clone 187.1; red), anti-Igλ (clone SL136; red), anti-CD169 (clone MOMA-1; green), and anti-CD22 (clone OX-97; blue).

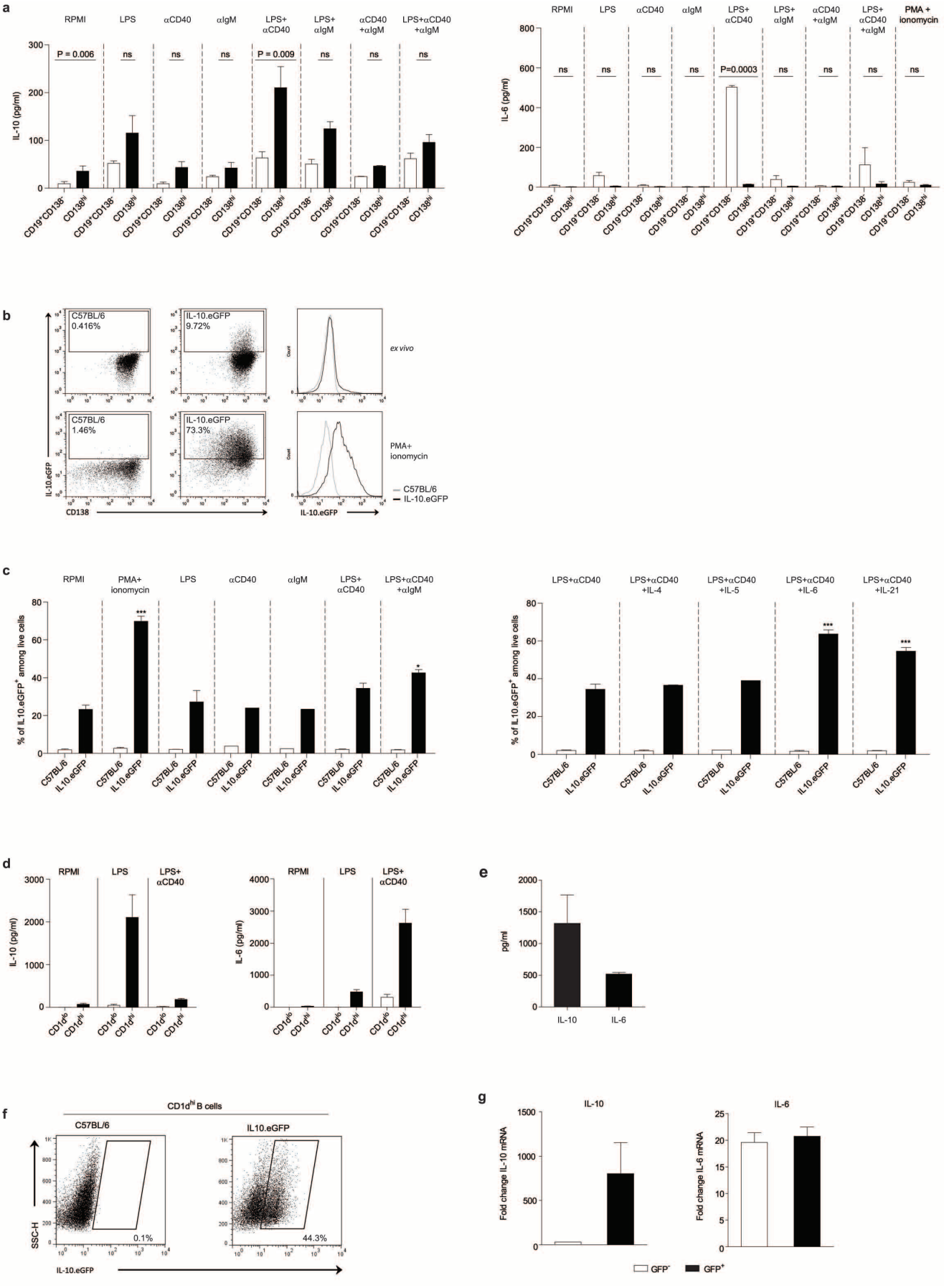

Extended Data Figure 8 | Production of IL-10 and IL-6 by plasma cells and B cells after *Salmonella* infection. **a**, $CD138^{hi}$ plasma cells and $CD19^{+}CD138^{-}$ B cells were isolated from spleen of C57BL/6 mice on day 3 after infection with attenuated *Salmonella* (SL7207; 10^7 c.f.u.), as described in Extended Data Fig. 6. Isolated cells were activated for 24 h as indicated with LPS (1 μg ml^{-1}), anti-CD40 (10 μg ml^{-1}), and anti-IgM (5 μg ml^{-1}). IL-10 (left) and IL-6 (right) concentrations were determined by Bio-Plex. Data shown are pooled from 2–5 independent experiments (mean ± s.e.m.). Results were compared using two-tailed unpaired *t*-test. *P* values > 0.05 are indicated by ns. **b**, **c**, $CD138^{hi}$ plasma cells were isolated from spleen of C57BL/6 or IL-10–eGFP mice on day 3 after infection with attenuated *Salmonella* (SL7207; 10^7 c.f.u.). **b**, Cells were analysed by flow cytometry directly after isolation to quantify IL-10–eGFP expression (*ex vivo*), and 24 h after re-stimulation with PMA plus ionomycin. Data show representative FACS plots and histogram overlays. Numbers in the plots indicate the percentages of IL-10–eGFP-positive cells among total live (PI^{-}) cells. **c**, Cells isolated from C57BL/6 and IL-10–eGFP mice were re-stimulated for 24 h, as indicated with LPS (1 μg ml^{-1}), anti-CD40 (10 μg ml^{-1}), anti-IgM (5 μg ml^{-1}), IL-4 (20 ng ml^{-1}), IL-5 (20 ng ml^{-1}), IL-6 (20 ng ml^{-1}) and IL-21 (20 ng ml^{-1}). Cells were analysed as in **b**. Data shown are pooled from 2–4 independent experiments (mean ± s.e.m.). Results were compared between condition RPMI and activated conditions (left) or between condition with added cytokine and condition LPS plus anti-CD40 (right) using one-way ANOVA followed by Bonferroni post-test (*$P < 0.05$, **$P < 0.01$; ***$P < 0.001$). **d**–**g**, Expression of IL-6 by IL-10-expressing $CD1d^{hi}$ B cells. **d**, $CD19^{+}CD1d^{hi}$ and $CD19^{+}CD1d^{lo}$ cells were isolated from spleen of naive C57BL/6 mice according to CD19 and CD1d expression using magnetic and FACS procedures, and stimulated for 24 h, as indicated. IL-6 and IL-10 concentrations in culture supernatants were determined by Bio-Plex. **e**, **f**, $CD1d^{hi}$ B cells were isolated from naive IL-10–eGFP mice and stimulated with LPS (2 μg ml^{-1}) for 48 h. IL-6 and IL-10 concentrations in culture supernatants were determined by Bio-Plex (**e**), and cells were analysed by flow cytometry to determine the frequency of IL-10–eGFP-expressing cells (**f**). **g**, $CD1d^{hi}$ B cells were isolated from naive IL-10–eGFP mice, and stimulated with LPS (2 μg ml^{-1}) for 48 h. IL-10–$eGFP^{-}$ and IL-10–$eGFP^{+}$ cells were then separated by FACS and analysed by real time PCR for expression levels of *Il10* and *Il6* mRNA. Data shown are pooled from two independent experiments (mean ± s.e.m.).

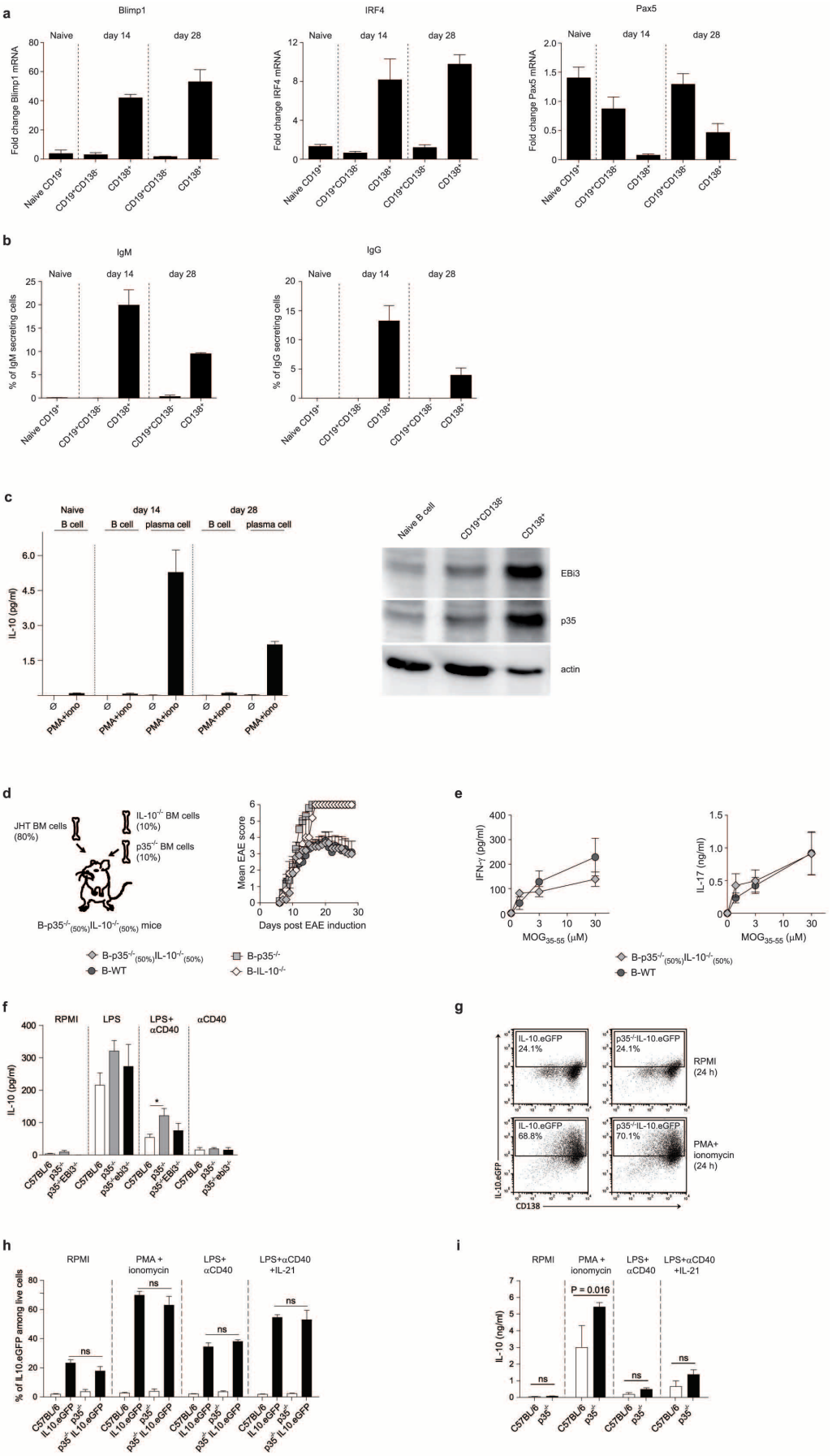

Extended Data Figure 9 | IL-35 and IL-10 production by plasma cells during EAE and *Salmonella* infection. **a**, B cells and plasma cells were isolated from spleens of mice on days 14 and 28 after EAE induction through magnetic and FACS procedures. Splenocytes were stained with anti-CD138-PE followed by labelling with anti-PE microbeads, and magnetic separation. The obtained CD138-positive and CD138-negative fraction were stained for CD19, CD138, and CD11b/CD11c/CD90/DAPI. $CD138^+CD11b^-CD11c^-CD90^-DAPI^-$ and $CD19^+CD138^-CD11b^-CD11c^-CD90^-DAPI^-$ cells were then isolated from CD138-positive and CD138-negative fractions, respectively, by FACS, as bulk cells. Naive splenic B cells (naive $CD19^+$) were isolated from unchallenged C57BL/6 mice by magnetic selection. *Blimp1*, *Irf4* and *Pax5* mRNA expression was quantified by real-time PCR. Data compile 2 independent experiments (mean ± s.e.m.). **b**, Production of IgM and IgG by plasma cells and B cells isolated from mice during EAE was determined by ELISPOT. A compilation of 3 independent experiments for day 14, and 2 independent experiments for day 28 is shown (mean ± s.e.m.). **c**, Left, $CD19^+CD138^-$ B cells (B cell) and $CD138^+$ plasma cells (plasma cell) were isolated from spleens of mice on days 14 and 28 after EAE induction through magnetic and FACS procedures, as described in **a**, and stimulated for 24 h with PMA plus ionomycin (PMA plus iono) or kept in medium (∅). IL-10 concentrations were determined by Bio-Plex. Data are pooled from 4 independent experiments for day 14 and 2 independent experiments for day 28 (mean ± s.e.m.). Right, B cells ($CD19^+CD138^-$) and $CD138^+$ plasma cells ($CD138^+$) were isolated from spleens of mice on day 14 after EAE induction through magnetic isolation. For this, splenocytes were stained with anti-CD138-PE followed by labelling with anti-PE microbeads, and magnetic separation to yield $CD138^+$ plasma cells. B cells were obtained from the CD138-negative fraction after further depletion of remaining $CD138^+$ cells, and positive selection using anti-CD19 magnetic microbeads. Purities were above 95%. Cell lysates were separated on SDS–PAGE gel and sequentially blotted with anti-EBI3, anti-p35, and anti-actin antibodies. Data show representative results of two independent experiments. **d**, **e**, Mice in which B cells cannot co-express IL-10 and IL-35 do not develop exacerbated EAE. **d** Left, $B^{p35^{-/-}}{}_{(50\%)}{}^{Il10^{-/-}}{}_{(50\%)}$ were obtained by reconstituting lethally irradiated recipient mice with BM cells from JHT mice (80%), IL-10-deficient mice (10%), and p35-deficient mice (10%). B^{WT} mice were produced using C57BL/6 BM instead of JHT BM cells. $B^{p35^{-/-}}$ and $B^{Il10^{-/-}}$ mice were obtained as outlined in Extended Data Fig. 10. Right, EAE was induced in $B^{p35^{-/-}}{}_{(50\%)}{}^{Il10^{-/-}}{}_{(50\%)}$ mice (grey diamonds, $n = 10$), $B^{p35^{-/-}}$ (grey squares, $n = 10$), $B^{Il10^{-/-}}$ (white diamonds, $n = 5$) and B^{WT} (dark grey circles, $n = 10$) mice. Data show clinical EAE scores. **e**, Splenocytes were harvested from $B^{p35^{-/-}}{}_{(50\%)}{}^{Il10^{-/-}}{}_{(50\%)}$ and B^{WT} mice on day 28 after EAE induction, and re-stimulated individually for 48 h with $MOG_{35–55}$. Culture supernatants were analysed by ELISA to determine concentrations of IFN-γ and IL-17. Data (mean ± s.e.m.) are pooled from two independent experiments. **f**, Production of IL-10 by IL-35-deficient B cells *in vitro*. Splenic B cells from naive C57BL/6, $p35^{-/-}$, and $p35^{-/-}Ebi3^{-/-}$ mice were stimulated with LPS (1 μg ml^{-1}), anti-CD40 (10 μg ml^{-1}), alone or in combination, as indicated, for 72 h, and IL-10 concentrations were determined by Bio-Plex. Data (mean ± s.e.m.) are pooled from three independent experiments. Results were compared between C57BL/6 cells and cells from mutant mice using one-way ANOVA followed by Bonferroni post-test (*$P < 0.05$). **g–i**, IL-35 is not necessary for production of IL-10 by $CD138^{hi}$ plasma cells during *Salmonella* infection. $CD138^{hi}$ plasma cells were isolated from spleen of C57BL/6, IL-10–eGFP, $p35^{-/-}$, and $p35^{-/-}$ IL-10–eGFP mice on day 3 after infection with attenuated *Salmonella* (10^7 c.f.u.) using a combination of magnetic and FACS methods. Cells were analysed by flow cytometry (**g**) to determine the frequency of IL-10–eGFP-expressing cells after re-stimulation as indicated for 24 h (**h**). Numbers in the plots indicate the percentages of IL-10–eGFP-positive cells among total live (PI^-) cells. Results were compared using two-tailed unpaired *t*-test. **i**, $CD138^{hi}$ plasma cells isolated from C57BL/6 and $p35^{-/-}$ mice were re-stimulated for 24 h as indicated. IL-10 concentrations were determined by Bio-Plex. Data are pooled from two independent experiments (mean ± s.e.m.). Results were compared using two-tailed unpaired *t*-test with Welch's correction. *P* values >0.05 are indicated by ns.

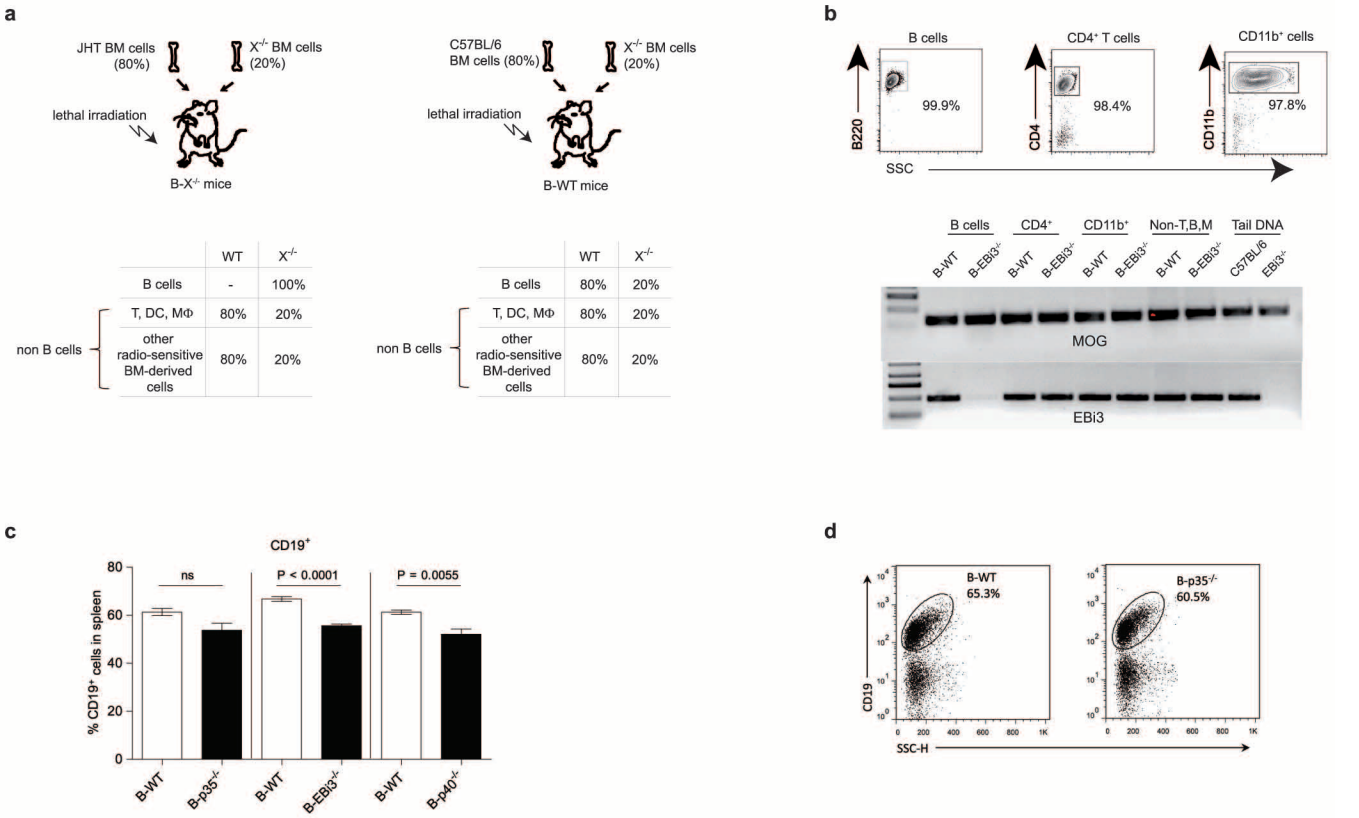

Extended Data Figure 10 | Generation and validation of bone marow chimaera. **a**, Scheme for the generation of $B^{X-/-}$ and corresponding control B^{WT} mice. Left, $B^{X-/-}$ mice with a deficiency in gene *X* restricted to B cells were obtained by reconstituting lethally irradiated recipient mice with a mixture of BM cells from B-cell-deficient JHT mice (80%) and from gene *X*-deficient ($X^{-/-}$) mice (20%). The table indicates the contribution of JHT and $X^{-/-}$ BM cells to relevant haematopoietic cell types in the resulting chimaera, taking into account that JHT mice carry wild-type (WT) alleles of gene *X*. In $B^{X-/-}$ mice, B cells only developed from $X^{-/-}$ BM cells and therefore were all $X^{-/-}$. In contrast, all other haematopoietic lineages developed from both $X^{-/-}$ and JHT BM cells. As the JHT and $X^{-/-}$ BM cells were injected in a ratio 80:20, most haematopoietic cells other than B cells carried a wild-type genotype for *X* in $B^{X-/-}$ mice. Right, the corresponding control B^{WT} mice were obtained by reconstituting lethally irradiated recipient mice with a mixture of BM cells from WT C57BL/6 mice (80%) and from $X^{-/-}$ mice (20%). The table indicates the contribution of WT and $X^{-/-}$ BM cells to relevant haematopoietic cell types in the resulting chimaera. In B^{WT} mice, all haematopoietic lineages, including B cells, developed from WT (80%) and $X^{-/-}$ (20%) BM cells. Therefore B cells mostly had a wild-type genotype in B^{WT} mice, which also controlled for possible effects owing to the 20% $X^{-/-}$ haematopoietic cells other than B cells present in $B^{X-/-}$ mice (for example, 20% $X^{-/-}$ T cells, and so on). **b**, Top, representative FACS plots of isolated B cells, $CD4^+$ T cells and $CD11b^+$ cells purified from naive $B^{Ebi3-/-}$ and B^{WT} mice, using magnetic and FACS-based methodologies; (bottom) genomic DNA was extracted from the sorted cell populations, including the non-labelled $B220^-CD4^-CD11b^-$ cells (indicated as Non-T,B,M). Genomic DNA samples from tail biopsies of C57BL/6 and $Ebi3^{-/-}$ mice were used as controls. The amounts of genomic DNA present in each sample were equilibrated using the *Mog* gene as standard. Using equilibrated samples, the wild-type *Ebi3* allele was detected by PCR in all DNA preparations except for B cells from $B^{Ebi3-/-}$ mice, and the tail biopsy from $Ebi3^{-/-}$ mice. **c**, Reconstitution of the B-cell compartment in BM chimaeric mice. $B^{p35-/-}$, $B^{Ebi3-/-}$, $B^{p40-/-}$ and corresponding B^{WT} controls were killed after reconstitution. Data show the percentage of $CD19^+$ B cells in spleen, as determined by flow cytometry. Data are pooled from 2–3 independent experiments. Data (mean ± s.e.m.) include $B^{p35-/-}$ ($n = 6$) and corresponding B^{WT} mice ($n = 7$), $B^{Ebi3-/-}$ ($n = 7$) and corresponding B^{WT} mice ($n = 9$), $B^{p40-/-}$ ($n = 7$) and corresponding B^{WT} mice ($n = 7$). Comparisons of B-cell reconstitutions between $B^{X-/-}$ and corresponding B^{WT} mice were done with two-tailed unpaired *t*-test with Welch's correction (*P* values > 0.05 are indicated as ns). **d**, Representative FACS plots of B cells from B^{WT} and $B^{p35-/-}$ mice. Cells are gated on live (PI^-) spleen cells.